In Vitro, Ex Vivo, Penetration (EpiDerm^{TM}) and in Vivo Dermatokinetics of Ketoconazole Loaded Solid Lipid Nanoparticles for Topical Delivery

Mohhammad Ramzan
Panjab University Institute of Pharmaceutical Sciences
Samuel Gourion-Arsiquaud
TRI, Princeton, New Jersy
Afzal Hussain
King Saud University College of Pharmacy
Jaspreet Singh Gulati
Hitech Formulations Pvt Ltd
Qihong Zhang
TRI, Princeton, New Jersey
Sonia Trehan
Rutgers University: Rutgers The State University of New Jersey
Vinam Puri
Rutgers University: Rutgers The State University of New Jersey
Bozena Michniak-Kohn
Rutgers University: Rutgers The State University of New Jersey
Indu Pal Kaur (indupalkaur@yahoo.com)
Panjab University Faculty of Pharmaceutical Sciences

Research Article

Keywords: Ketoconazole loaded SLNs, Design Expert, In-vitro and ex-vivo studies, In-vivo investigations, EpiDermTM model

Posted Date: May 18th, 2021

DOI: https://doi.org/10.21203/rs.3.rs-408418/v1

Abstract

The study focused to optimize, evaluate and investigate mechanistic perspective of ketoconazole (KTZ) loaded solid lipid nanoparticles (KTZ-SLNs) for enhanced permeation across rat skin. KTZ-SLNs were evaluated for size, distribution, zeta potential (ZP), percent entrapment efficiency (%EE), drug release, morphology, thermal behavior (DSC), compatibility (FTIR) and solid state characterization (X-ray diffraction, XRD). Moreover, ex-vivo permeation and drug deposition into rat skin were conducted using Franz diffusion cell. Mechanistic evaluations were confirmed using confocal laser scanning microscopy and vibrational ATR methods using EpiDerm^{TM} model. An in vivo dermatokinetics study was performed to ensure KTZ access to the dermal region. Accelerated and photostability studies were conducted at different temperatures (0, 30, and 40 °C) for 12 months. The spherical optimized KOF1 showed optimal particle size (291 nm), and high negative ZP (-27.7 mV). Results of FTIR, DSC, and XRD confirmed compatibility of KTZ with excipients, purity of KTZ & dissolved KTZ in lipid matrix, and amorphous nature of KTZ-SLNs. In-vitro release was found to be slow and sustained whereas ex vivo permeation parameters were significantly high in KTZ-SLNs as compared to drug suspension and marketed product. Drug retention was 10- and -5 fold higher than KTZ-SUS and marketed product, respectively. Pharmacokinetic parameters were improved by SLNs formulation. Confocal raman spectroscopy experiment showed that KTZ-SLNs could penetrate beyond the human stratum corneum into viable epidermis. Fluorescent microscopy confirmed improved penetration of KTZ-SLNs was through human follicular pathway. KTZ-SLNs stable over 12 months under set conditions.

Introduction

Superficial fungal infections are common worldwide and constitute one-fourth of common skin infections caused by dermatophytes. The dermatophytes are responsible to invade the keratinized tissue of stratum corneum (SC) [1]. These have severe psychological, social and financial consequences for patients [2]. Most fungal infections reside in the lower epidermal and dermal regions and the vellus hair. These regions are inaccessible to the conventional antifungal formulations due to inadequate dose of the drug reaching to the target site. Most fungal cells have specialised efflux system resulting in frequent drug resistant. Sub-optimal concentration of antifungal agents at the site of infection, poor compliance to therapy, poor delivery modalities, and active antifungal efflux are responsible for frequent recurrence, chronic fungal infections and most seriously to drug resistance. Dermatophytes causing intracellular are critical to treat due to long term therapy and patient incompliance [3]. Topically administered KTZ is clinically recommended to control dermal fungal infections. It is a broad-spectrum antifungal agent to treat skin related candidiasis, tinea, and related dermal infections. Moreover, the drug is potential to control cutaneous superficial (*Candida*, and *Malassezia*), localized, and secondary infections such as androgenic alopecia, leishmaniasis, and yeast induced blepharitis [3].

KTZ is lipophilic drug (log P = 4.74) with poor aqueous solubility (0.04 mg/ mL) [4]. The drug is sensitive to light and possessed photo degradation. KTZ is reported to cause several undesirable effects [5] (nausea, vomiting, gastrointestinal disturbance and hepatotoxicity) after oral administration.

Conventional creams are associated with limited drug access to the target site, common side effects (swelling, irritation/redness, itching, and contact dermatitis) and poor therapeutic efficacy to control deeper infection of skin [6]. In literature, several approaches have been published by formulating in various novel nanocarriers. However, these in-vitro and ex-vivo studies (using animal model) overestimated to simulate in-vivo performance of the drug. There is lack of in-vivo data to confirm and simulate in-vivo performance of the drug in animal model to human body. No report has been published for comprehensive in-vitro, ex-vivo, and in-vivo studies of KTZ loaded lipidic nanocarrier using animal and human cadaver to rationalize improved efficacy of KTZ ferrying SLNs.

Solid lipid nanoparticles (SLNs) are well explored nanomedicine to improve solubility and therapeutic efficacy of several potential antifungal agents. KTZ is reported for topical delivery by tailoring vesicular systems, micelles and nanoemulsion [6–8]. These nanocarriers are either physically unstable or toxic due to retained organic solvent in final product [6–8]. Moreover, these nanocarriers are associated with limited drug loading, release issue, cost of the product, and scale up for large scale production. Unentrapped drug may cause skin irritation on topical application. In contrast, SNLs prepared by high pressure homogenization is scalable with several obvious benefits such as increased drug solubility in lipid matrix, drug protection (stability and photostability), high drug loading, maximized cellular internalization of candida cells, reduced efflux based drug resistance and reduced skin adverse reactions [9]. Biocompatible SLNs may enhance skin permeation, drug deposition, penetration and reduced recurrence of disease.

In this study, we optimized SLNs formulation using experimental design tool and characterized for in-vitro parameters (particle size, size distribution, shape, zeta potential, solid state properties, and in-vitro drug release). Moreover, the optimized formulation was studied for ex vivo (rat skin and human cadaver) and in-vivo performance in rat model. Long term stability study at different temperatures and photo-stability ensured the success of the product over a period of one year.

Materials And Methods

Materials

Ketoconazole (KTZ) was procured from a local pharmaceutical industry (Velite Pharmaceuticals, Ludhiana, Punjab, India). Phospholipon 90G and compritol 888 ATO (CATO) were obtained gift samples from Lipoid (Germany) and Gattefosse (France), respectively. Polyethylene glycol 400 (as cosolvent) and tween 80 (as surfactant) were received from CDH, Mumbai (India). Millipore water was used as aqueous solvent wherever required in the study. Fluorescence dye (fluorescein sodium) was purchased from Sigma Aldrich (Mumbai, India). All chemicals were of analytical grade.

Methods

Preliminary screening studies

Several batches of blank formulations were prepared to screen excipients such as solid lipid (Compritol® 888 ATO), surfactant (tween 80), cosolvent (polyethylene glycol 600) (PEG 600), and stabilizer (phospholipon 90G (P90G). Taguchi design was applied for factors and levels. Several variables (run cycles, speed and stirring time) of high pressure homogenization (HPH) technique were optimized to get stable SLNs (overnight benchtop stability).

Formulation method to load ketoconazole in solid lipid nanoparticles (KTZ-SLNs)

Preliminary study was carried out to select excipients and their levels (low and high). Based on benchtop stable product, the higher and the lower levels of factors were decided to feed as input parameters in experimental design software (Design Expert). The lipid organic phase was composed of CATO, PEG-600, and KTZ (fixed amount) which was heated to melt at 75°C. Similarly, the aqueous phase contains tween-80 and P90G previously set at the same temperature. The aqueous phase was stirred at high speed (1000 rpm) using stirrer (WiseTis, HG-15D, Daihan, Korea). The hot organic phase was slowly added to the aqueous phase under constant stirring to result in a coarse emulsion. The prepared coarse emulsion was passed through a high pressure homogenizer (HPH) (EmulsiFlex-C3, Avestin, Canada), at 1000 bar pressure for 7 cycles. The formed o/w emulsion was cooled to room temperature to achieve KTZ loaded SLNs (2% w/v). Thus, several batches of formulations were formulated as per dictated in experimental design (central composite design). In case of fluorescein sodium dye probed KTZ-SLNs, the same procedure was adopted and except dye was dissolved in aqueous phase.

Optimization process

Experimental protocol was designed to evaluate the critical factors and their significant levels to get the most robust formulation with optimal content of lipid (CATO) and tween 80 (surfactant). A central composite design (CCD) with α=1.414 was run in the Design Expert (version 8.0.1 Stat-Ease Inc. USA) [7]. CATO (X_1) and tween 80 (X_2) were selected as independent variables (factors). Similarly, mean particle size (Y_1), %EE (Y_2) and total drug content (Y_3) were responses (dependent variables). In optimization process, total 13 runs were experimented at 5 levels (-α, -1, 0, +1, +α). A general polynomial mathematical quadratic equation was generated to quantify and establish a correlation between the independent (X) and dependent variables (Y):

$$Y=\beta_0 + \beta_1 X_1 + \beta_2 X_2 + \beta_3 X_1 X_2 + \beta_4 {X_2}^2 + \beta_5 {X_2}^2$$

Where Y is dependent variable with two coefficients (β_1 & β_2) of factors (X_1 & X_2). β_0 is an intercept. β_3 is a coefficient of interaction between factors X_1 and X_2, whereas β_4 and β_5 are the coefficients of quadratic terms "X_1" and "X_2", respectively. Positive and negative signs indicate synergistic and antagonistic effect

of factors on the response, respectively. ANOVA (analysis of variance) provides parameters (F, *p*, and r^2 values) to validate the model applied for optimization process using the experimental design.

Characterization of KTZ loaded suggested SLNs formulations

Measurement of particle size, polydispersity index, and zeta potential

Particle size, size distribution and surface charge are critical factors to control in-vitro and in-vivo performance of product. Particle size and PDI were measured using photon correlation spectroscopy (PCS) technique which is based on the principle of light diffraction phenomenon. The sample was previously diluted with water (50 fold) for analysis (Beckman Coulter, Delsa™ Nano C, USA). Zeta potential of KTZ- SLNs dispersion was measured without sample dilution (Beckman Coulter, Delsa™ Nano C zetasizer, USA) at 25ºC and the electric field strength of 23.2 V/cm. Experiments were replicated for mean and standard deviation (n = 3).

Percent total drug content (%TDC) and entrapment efficiency (%EE)

KTZ-SLNs formulations contain 2%w/v of KTZ. Formulation (1 mL) was dissolved in chloroform: methanol mixture (2:1). The mixture of organic solvents were able to dissolve and disrupt solid lipid of tailored KTZ-SLNs. The mixture was filtered and the content of KTX was quantified using validated HPLC method. % EE was determined by dialyzing KTZ-SLN dispersion (1 mL) in a dialysis membrane (14K Da MW cut-off) immersed in 50 mL ethanol and stirred magnetically. After 1h KTZ-SLNs were removed from the bag, disrupted with suitable quantity of chloroform: methanol mixture (2:1) and amount of drug was determined by HPLC. The dialysate was decided based on the assumption that the entire quantity of unentrapped can dissolve in a suitable quantity (50 mL) in an appropriate time (≥1h) to accurately determine amount of unentrapped drug.

Desirability function

The desirability parameter was used to identify and evaluate the optimized formulation by experimental design. Mathematically, this is a numerical function parameter to identify possible interaction between factors. Moreover, it depends upon the set conditions of optimization process such as goal and importance given to each dependent and independent variables. The value of desirability function varies from zero to unity. Zero indicates the model is not fit and out of optimization whereas the value

approaching to unity indicate the best fit of the model applied for optimization. The significant terms ($p < 0.05$) were chosen for final equations. The model was considered to be the best fit when the actual correlation coefficient (r^2) value was close to the adjusted correlation coefficient (adjusted r^2). Selected formulations of KTZ-SLNs were prepared from the design space and used as checkpoints to assess the prognostic behaviour of the developed mathematical model.

Preparation of ketoconazole suspension (KTZ-SUS)

KTZ suspension (KTZ-SUS) was prepared by method described before with slight modification [8]. An accurately weighed amount of KTZ was dispersed in water containing 1% w/v of tween 80 as surfactant and sodium salt of carboxymethyl cellulose (0.1%w/v) as suspending agent. The drug was rigorously stirred for 60 min in the aqueous phase to obtain a stable suspension with optimal consistency. Final strength of the suspension was equivalent to commercial product (2% w/v). This product was used in the further studies as control.

Thermal behaviour of the formulations

The thermal behaviours (fusion temperature and fusion enthalpy) of pure and formulations were assessed using a differential scanning calorimeter (DSC). A weighed amount (2 mg) of the samples (Lipid, KTZ, KTZ-SLNs, Blank SLNs) was placed in an aluminium pan and heated at a fixed heating rate (10°C/min) till 300°C using DSC (821e Mettler Toledo, Switzerland). The generated thermograms were analysed, and marked for the values of any significant shift or disappearance/appearance of new peaks. The calorimeter was calibrated by pure Indium (melting point) for nitrogen flow and heating rate. Nitrogen gas was used at a purging rate of 50 mL /min.

Compatibility study using Fourier Transform Infra-red (FT-IR)

To negate any chemical interaction of the drug with explored excipients, the sample alone (KTZ) and formulations (KTZ-SLNs, and placebo SLNs) were subjected for FT-IR analysis. The FT-IR spectrometer (Agilent Technologies 630 Cary) was run for the sample using pellet method. A small amount of the sample was physically mixed with KBr followed by pellet formation. The pellet was processed for characteristic peaks using Micro Lab software. The samples were scanned over the range of 4000- 400 cm^{-1}.

Solid state behaviour using powder X-ray diffraction (XRD) method

The prepared SLNs formulations were solid in nature and considered for improved solubility of the drug in solid matrix. In general, crystalline materials exhibit characteristic peaks in XRD graph. Therefore, it was required to assess solid state behaviour of the developed formulation. This was confirmed by analysing the nature of formulated nanoparticles using XRD (XPERT-PRO, PANalytical, Netherlands). KTZ-SLNs and blank SLNs dispersions were lyophilized prior for the analysis. The test sample was exposed to CuKα radiation (45 kV, 40 mA) with scanning angle ranged between 5° and 50°. The values of 2θ and scanning step time were 0.017° and 25s, respectively. Pure drug, lyophilized KTS-SLNs, blank SLNs (without drug) were analysed.

Surface morphology analysis

Surface morphology of prepared solid lipid nanoparticles (KTZ-SLNs) was examined by high resolution transmission electron microscopy (HR-TEM) and field emission scanning electron microscopy (FE-SEM). Prior to observation under HR-TEM and FE-SEM, KTZ-SLNs were diluted (50 X) with distilled water. The procedure for FE-SEM observations including placing the KTZ-SLNs dispersion on Nucleopore Track-Etch membrane and drying at room temperature. Dried membrane was attached to the silicon wafer using double sided carbon tape followed by sputter coating with gold under FE-SEM (FE-SEM SU8000, Hitachi, Japan). For HR-TEM KTZ-SLNs was stained (0.2% w/v of phosphotungstic acid) during 5 min in phosphate buffer at pH 6.8. Then, the excess phosphotungstic acid was removed using a filter paper. The stained sample of KTZ-SLNs was spread over carbon coated copper grid and was observed under HR-TEM (H-7500, Hitachi, Japan) at a voltage of 200 kV, for morphology (shape and size).

Release behaviour and mechanism

In-vitro release pattern of optimized formulation was studied using a dialysis membrane as per reported method [9-10]. A fixed volume (1 mL) of KTZ-SLNs and KTZ-SUS containing 20 mg of KTZ was loaded in the dialysis membrane (molecular weight cut-off of 12KDa). The dialysis membrane was soaked in water for 12 h before experiment. The dialysis membrane containing sample was suspended in a release medium (phosphate buffer solution, pH 7.4). Sink condition was maintained using dimethyl sulfoxide (DMSO). Sampling (2 mL) was carried out at various time points (1, 2, 4, 8, 12, 16, 24, 48, and 72 h). The withdrawn volume was replaced with fresh release medium (equal volume) at each time points. The sample withdrawn was filtered and analysed using validated HPLC method at λ_{max} of 210 nm. Analysis was replicated for mean and standard deviation (n=6). Finally, various mathematical models were applied to investigate release mechanism (zero order, first order release, Higuchi model and Korsmeyer-Peppas model).

Drug permeation and deposition studies: Ex vivo performance across rat skin

Permeation potential and drug deposition were carried out using Franz diffusion cells as per reported method [11]. The optimized SLNs formulation was compared against drug suspension and marketed product. For this, rat skin (abdominal) was made free of hairs using digit trimmer without making any surgical cuts or injury. The excise and trimmed skin was placed between two chambers of Franz diffusion cell such that the upper layer faces the formulation and inner layer towards the receptor medium (PBS, pH 7.4). The receptor chamber was filled of release medium (30 mL) and set at 32±1°C under constant stirring using teflon coated magnetic bead [12]. The test sample (0.5 mL containing 10 mg of KTZ) was placed over exposed skin (available surface area of 2.1 cm^2). Three samples (KTZ-SLNs, KTZ-SUS and KTZ-MKT) were studied separately under similar experimental conditions. The donor chamber was properly covered with paraffin film to avoid loss of solvent or dryness of the sample. The sampling was performed at different time points (0.5, 1, 2, 4, 6, 8, 12, 24, 48 and 72 h) followed by replacing equivalent volume of withdrawn sample with fresh release medium. Notably, DMSO (5%) was added to the receptor medium to maintain sink condition. The withdrawn sample was filtered using membrane filter (0.2 µm). The permeated amount of the drug across the skin was estimated using HPLC. Several permeation parameters (cumulative amount of drug permeation, permeation flux, and enhancement ratio) were calculated [13]. After completion of permeation study, the skin samples were removed and washed with running water for drug deposition (retention) study.

Skin retention studies

This study is an extension of the skin permeation study. After completion of the permeation study, the skin was washed with running water to remove adhered treated sample. Then, the skin was sliced into small pieces using surgical scissor and placed in a solution containing methanol and chloroform (2:1 ratio) [14]. The drug deposited or retained in the skin was extracted over 12 h under constant stirring at room temperature. Then, they were filtered and the filtrate was centrifuged (9000 rpm) for 15 min to get the supernatant. The obtained supernatant was analysed for the permeated amount of the drug using HPLC. The study was repeated for mean and standard values.

Dermatokinetics: An in-vivo study

The animal study was carried out in Wistar albino rats weighing about 250-300 g of both sexes. They were get issued from Institutional animal house UIPS (University Institute of Pharmaceutical Sciences) (Approved as regd. No. 45/GO/ReBiBt/S/99/CPCSEA). All of the animals were housed in conditioned room with free access of food and water as per guideline. Animals were randomly selected and grouped (n=6 per group) as per treatment schedule. The body surface of rats was properly inspected for any possible injury and abnormality. The dorsal surface was used to locate a site of application by making three areas (3 cm^2) free of hairs. Each group received all three formulations at labelled location on the dorsal site. After 24 h of shaving, formulations (KTZ-SLNs, KTZ-SUS and KTZ-MKT), were applied with equivalent concentration and dose strength. Rat was ethically sacrificed at varied time points (2, 6, 12, 24,

48 and 72 h) for dermatokinetic study. Three skin samples were excised from the applied site and washed water to remove adhered content. Then, the skin samples were sliced into small pieces to extract the drug content by dispersing in a mixture of chloroform and methanol (2:1). The mixture was homogenized after 8 h and filtered. The filtrate was centrifuged to get a supernatant. The supernatant was used to estimate the extracted amount of the drug by HPLC method. The data obtained was fitted into one compartment open model. For dermatokinetics profile, the drug concentration versus time profile was estimated presented as a graph using a PK solver (version 1.1). Several dermatokinetics parameters such as area under the curve (AUC_0-_{72} and $AUC_{0-\infty}$), the maximum drug concentration reached in the skin layer (C_{max}), the time required to attain C_{max} as T_{max} were assessed.

Fluorescence microscopy study on human dermatome skin (EpiDerm^{TM})

This was conducted to visualize the permeated KTZ tailored in SLNs using EpiDerm^{TM} as a skin model (MatTek Corporation, Ashland, USA). Fluorescein probed SLNs (F-SLNs) was prepared as per method discussed before. Approximately 30 μL of 2 % aqueous solution of fluorescein (aqueous solution) was taken as control and topically applied to the surface of EpiDerm^{TM}. Fluorescein was excited at 470 nm and the fluorescent emission was detected at 515 nm. Several representative images of the treated skin were visualized for mechanistic evaluation using fluorescent microscopy (IX71 Olympus Inverted Microscope, Olympus, Tokyo, Japan) at 2 h and 24 h with a 10X magnification.

Vibrational spectroscopic imaging techniques in human skin

Skin treatment procedure

Flash-frozen human skin with thickness 4cm^2 (T-SKN-FF2CM) purchased from licensed supplier (ZenBio Inc, USA) was used for this study. All of the skin samples used in this study were from the same donor. 2.5 cm x 2.5 cm piece of skin was cut and cleaned. Formulations (KTZ-SLNs and KTZ-SUS) were applied topically on the skin surface in excess. Product was massaged on the skin using a glass rod and allowed to sit for 5 min. Skin was placed on a Franz diffusion cell for 3 and 24 h at 32°C. After 3 and 24 h, the excess product on the skin surface was gently blotted with a wet kimwipe. To evaluate product penetration inside the skin, sample preparations were used. Transverse skins sections (8 µm) were obtained using cryo-microtome and scanned by ATR-FTIR imaging to visualize product penetration inside the different skin layers. Skin cross-sections (8µm) were cut using a cryostat. These cross-sections were scanned by ATR-FTIR imaging to evaluate product penetration inside the epidermis. ATR-FTIR images of the cross sections were recorded with a Spotlight 400 System (Perkin Elmer Instruments, Shelton, Conn.,

USA), consisting of a FTIR spectrometer with a mercury-cadmium-telluride (MCT) focal plane array detector. Images were collected in reflective mode at a spectral resolution of 4 cm^{-1} and 4 scans accumulations in the mid-infrared (MIR) region between 4000 and 750 cm^{-1} with a spatial resolution of 6.25 x 6.25 µm at room temperature (24°C). The ATR imaging accessory used a germanium crystal placed directly in contact with the skin samples. All the data were processed (baseline correction, generation of spectroscopic parameters) using GRAMS/AI (Thermo Fisher Scientific) or ISys software from Spectral Dimensions (Olney, MD).

Confocal Raman spectroscopy imaging

Skin was also scanned by confocal Raman spectroscopy to evaluate product penetration inside the stratum corneum and beyond in the epidermis. Human skin was treated for 24 h at 34°C. After incubation, skin was placed in a home-built brass cell. Confocal Raman images were acquired with a WITec Alpha-3000R plus confocal Raman microscope (Ulm, Germany) equipped with a 532nm laser. XZ images were taken for each sample. The XZ depth image was typically 50x30$µm^2$ covering SC and upper viable epidermis (VE) region with 4 µm steps and a 20 second exposure time.

Stability studies

Photostability

It was conducted for KTZ-SLNs and KTZ-SUS as per ICH guidelines Q1B [15]. The freshly prepared samples were packed in amber coloured clear glass vial, labelled and recorded for further process. Each batch was exposed to illumination light of 1.2 million lux h and an integrated near UV energy (200 watt h/m^2) for 10 days in a photostability chamber (Binder Gmbh, Germany).

Long term accelerated stability

A long term accelerated stability of the developed formulations (KTZ-SLNs) were conducted as per ICH Q1A guidelines [16] . A constant amount of each formulation was transferred to fresh and clean amber colour glass container. Three batches for each formulations were prepared, packed and labelled as per experimental schedule [(2-8 ^{0}C, 30 (±2°C)/65% (± 5%) RH and 40 (±2°C)/75% (±5%) RH]. The samples were withdrawn at 0, 30, 90, 180, and 360 days, and evaluated for particle size, % EE, and the drug content (%).

Results And Discussion

Preparation of formulation and pre-optimization

Initially, several trial formulations were prepared using the investigated lipid (CATO as lipid), surfactant (tween 80), co-surfactant (PEG600) and stabilizer (P90G) as per Taguchi design (Table 1). Moreover, the design was used to select factors and levels (Table 1). Several trial formulations were prepared by varying run cycles, speed and time for homogenization using HPH as shown in Table 1.

Table 1
Taguchi design variables

		Level		
Code	**Factor**	**−1**	**(+1)**	**Response**
A	Lipid (g)	2.0	3.0	Particle size (nm)
B	Tween 80 (g)	0.6	1.4	Entrapment efficiency (%)
C	PEG600 (g)	0.4	1.2	
D	Phospholipon 90 G (g)	0.01	0.03	
E	Stirring speed (rpm)	8000	10000	
F	Stirring time (min)	8	10	
G	Homogenization Cycle	5	7	

Std	**Run**	**A**	**B**	**C**	**D**	**E**	**F**	**G**
5	1	5.6	2.1	4.2	0.3	8000	8	5
1	2	5.6	2.1	1.2	0.3	10000	10	7
7	3	5.6	4.9	4.2	0.1	8000	10	5
4	4	7.0	4.9	1.2	0.3	8000	8	5
3	5	5.6	4.9	1.2	0.1	10000	8	7
6	6	7.0	2.1	4.2	0.1	10000	8	5
8	7	7.0	4.9	4.2	0.3	10000	10	7
2	8	7.0	2.1	1.2	0.1	8000	10	7

The formulation exhibiting benchtop stability for overnight was selected for selecting lower and higher levels of each factor for Design Expert (central composite design) (Table 2).

Table 2
Optimization (central composite design)

Level of factors					
Code and factors	-α	-1	0	+ 1	+α
X_1:CATO (g)	1.5	2.0	2.5	3.5	4.0
X_2:Tween 80 (g)	0.3	0.7	1.1	1.4	2.1
Constraints					
Code and responses		**Low**	**High**	**Goal**	
Y_1: Particle size (nm)		291.5	843.2	Minimum	
Y_2: EE (%)		35.5	84.6	Maximum	
Y_3: Total drug (%)		77.9	96.2	Maximum	
Formulation code	**X_1**	**X_2**	**Y_1**	**Y_2**	**Y_3**
KTZ–SLN1	+ 1	+ 1	391.5 ± 12.5	60.7 ± 0.42	78.6 ± 1.4
KTZ–SLN2	−1	−1	780.8 ± 13.2	35.5 ± 0.61	75.5 ± 1.7
KTZ–SLN3	0	0	453.6 ± 9.1	66.7 ± 0.57	80.1 ± 0.9
KTZ–SLN4	−1	+ 1	291.5 ± 6.3	84.6 ± 0.32	96.2 ± 1.3
KTZ–SLN5	0	−α	843.2 ± 17.2	42.6 ± 0.49	83.4 ± 1.5
KTZ–SLN6	0	0	450.4 ± 13.7	62.4 ± 0.51	85.6 ± 0.8
KTZ–SLN7	+ 1	−1	821.5 ± 19.6	67.4 ± 0.31	88.7 ± 1.4
KTZ–SLN8	+α	0	492.6 ± 8.2	66.3 ± 0.51	81.5 ± 1.7
KTZ–SLN9	0	0	449.8 ± 9.3	62.6 ± 0.38	80.1 ± 1.5
KTZ–SLN10	0	+α	424.8 ± 11.5	76.7 ± 0.41	82.3 ± 1.1
KTZ–SLN11	0	0	457.4 ± 7.9	62.5 ± 0.61	84.4 ± 0.9
KTZ–SLN12	0	0	455.2 ± 10.2	64.3 ± 0.55	85.6 ± 1.2
KTZ–SLN13	−α	0	635.2 ± 7.5	45.60 ± 0.4	79.4 ± 0.7
Composition and statistical analysis of KOF1					
KOF1 as optimized formulation					
X_1: 2.0 (g)					

Level of factors					
X_2: 1.4 (g)					
Response	**Model**	**r^2**	**Adjusted r^2**	**f value**	**p value**
Particle size (Y_1)	Quadratic	0.991	0.982	21.97	0.0006
%EE (Y_2)	Quadratic	0.9766	0.9842	19.68	0.0008
Total drug (Y_3)	Quadratic	0.9878	0.9791	8.80	0.0009
Generated polynomial equations					
$Y_1 = 2615.98 - 354.27X_1 - 416.84X_2 - 17.16X_1X_2 + 32.34X_1^2 + 52.26X_2^2$.					
$Y_2 = -173.36 + 51.95X_1 + 14.64X_2 - 1.42X_1X_2 - 2.85X_1^2 + 0.43X_2^2$					
$Y_3 = 134.38 - 19.35X_1 - 7.91X_2 - 1.23X_1X_2 + 1.78X_1^2 + 0.19X_2^2$					
Optimized KOF1			Y_1 (nm)	Y_2 (%)	Y_3 (%)
Observed value			293	88.5	96.25
Predicted value			289	84	95

We selected X_1 (CATO as lipid) and X_2 (tween 80) as independent factors at three levels as shown in Table 2. The set responses were Y_1, Y_2, and Y_3 for particle size (nm), %EE, and the drug content (%), respectively. This tool is reliable to obtain the most robust formulation with optimum content of the solid lipid and surfactant under set desired goals. Moreover, the software was used to identify the potential factors affecting dependent variables (Y_1-Y_3) and possible interaction between factors (X_1 and X_2). The central composite design (CCD) suggested thirteen formulations under given set of constraints and goal. The suitability of the model was assessed by analysis of variance (ANOVA). The statistical parameters (*p*, F, and r^2 values) were carefully examined for the model to be fit. All responses (Y_1-Y_3) followed quadratic model and the generated polynomial equations are presented in Table 2. The negative and positive signs associated with each term represent antagonistic and synergistic influence of individual factor on the investigated responses, respectively.

Particle size (Y_1) of SLNs dispersion is a significant parameter for efficient *in-vitro* and *in-vivo* experiments. The nanoscaled safeguard circumvents direct interaction of KTZ with efflux proteins thus ensuring its entry into the fungal cells. Furthermore, lower particle size reduces the tendency of coalescence which leads to increase in stability and shelf life of KTZ-SLNs formulation. The polynomial equation for Y_1 is given in Table 1 where negative signs of coefficients associated with both factors X_1 and X_2 indicate that these factors need to be reduced to get desired response. The 3- and 2-dimensional contour plots for Y_1-Y_3 are illustrated in Fig. 1A-B. The result showed that Y_1 increases with increase in X_1

(CATO) which may be due to higher content of lipid (Fig. 1A). Therefore, it should be reduced to an optimal level. In contrast, Y_1 was found to be decreased with decrease in tween 80 content first then increased on further reduction in X_2. Thus, both X1 and X2 need to be optimized to get the most robust SLNs. The lower value of *p* (0.0006) and high F (18.97) value confirmed the best fit of the model adopted for analysis of Y_1. Moreover, the adjusted correlation coefficient (r^2) was close to the observed value which suggested good fit of the model. The optimum particle size (minimum) was due to relatively higher concentration of surfactant (2.0 g) and optimal lipid content (1.4 g). However, with further increase concentrations of both the factors, there was increase in particle size due to micelles formation. Hence, it may conclude that to obtain optimized formulation, the optimum levels of X_1 and X_2 have to be required.

For Y_2, the positive signs of X_1 and X_2 associated with first and second terms of the quadratic equation (Table 2) suggested that the concentrations of X_1 and X_2 should be at high level for the optimized product. Thus, the effect of the concentration of lipid and tween 80 is directly proportional to Y_2. These two were found to be considerable factors to use in optimal concentration. The result is exhibited in in Fig. 1C-D (response surface and 2-D contour plots) where Y_2 was found to be linearly increased on increasing the content of X_1 which may be due to increased solubility of lipophilic KTZ in lipid. Compritol®888 ATO is a complex lipid composed of mixtures of mono, di, and triglycerides which form less perfect crystals, and accord space to accommodate drug molecules [17]. Furthermore, Y2 was found to be increased with increasing content of twee 80 (X_2). Statistical analysis suggested that the model was the best fit for this response as evidenced with high value of F (483.32), low p value (0.0001) and the closeness of r^2 between adjusted (0.9542) and predicted (r^2 = 0.9266) values. The generated quadratic equation is presented in Table 2 with associated coefficients in each terms. As Y_3, it is required to assess the totoal content of the drug present in the final formualtion. The total drug content is significant parameter for assessing stability and shelf-life of the formulation. It was expetced that the drug content (Y_3) shopuld increase with increase in X_1 and X_2 due to drug solubility in lipid and surfactant based improved emulsification. The drug content was the highest when both the factors (X_1 and X_2) were at axial point (X_1:+1 and X_2: +1) (Fig. 1E-F). The mathematical relationship of Y_3 to factors is represented by the quadratic equation obtained and presented in Table 2. When the lipid and tween 80 concentrations were held at central point (X_1 = 2.0 g and X_2 = 1.4 g) total drug content of KTZ loaded in SLNs (KTZ-SLN4) as in Table 2 had shown a maximal value of 96.2%. The model was significant ($p < 0.00087$) and fit as evidenced with the correlation coefficient (regular r^2 = 0.95) and adjusted r^2 (0.90).

Optimization and validation parameter

Based on statistical parameters for the responses Y_1-Y_3, the most robust formulation was obtained with optimum content of X_1 and higher content of X_2 to achieve the set goal. The predicted and observed values were closely related as evidenced with correlation coefficient value (r^2 ≥ 0.97) all explored responses (Y_1-Y_3) (figure 2A-C). There were no observed interaction for Y_1 and Y_2 (figure 2D-E). However,

the response Y3 exhibited a slight interaction between factors (figure 2F). The value of overall desirability function was obtained as 0.907 close to unity. Thus, the used model was the best fit under given set of experimental conditions and importance to each factor and response. The most optimized formulation obtained was KOF1 with the highest desirability function parameter as compared to other suggested formulations (figure 3).

Post-optimization studies: Evaluation parameters of KOF1

Particle size, PDI and zeta potential

The finally optimized formulation KOF1 was comprised of X_1 (2.0 g) and X_2 (1.4 g) with maximum desirability value. The results of particle size (Y_1), PDI, and zeta potential were found as 293 ± 6 nm, 0.258 ± 0.07 and -22.92 ± 2.4 mV, respectively, for KOF1 (table 2). Moreover, the result of %EE (Y_2) and % total drug content (Y_3) were found to be as 88.5 ± 1.5% and 96.25 ± 0.85% for KOF1, respectively. Notably, the total drug content of KTZ in final formulation of SLNs was 0.2% in our previous report published for ocular delivery **[8].** The present study was intended for topical delivery of KTZ to control fungal infections caused by the resistant and sensitive strains residing into the deeper dermal tissue. Therefore, higher strength (2%) was formulated and evaluated for in- vitro, ex- vivo and in-vivo performance as compared to marketed and prepared suspension. The predicted values of particle size, %EE and % drug content were 289.0 nm, 84%, and 95%, respectively for KOF1 suggesting good agreement of the model fit due to closeness of the predicted values to the observed values.

Differential scanning calorimetry (DSC)

Melting (heating) of lipid and recrystallization (cooling) of hot lipidic emulsion after passing through HPH to form solid lipid nanoparticles may change the crystalline behaviour as well as the polymorphic form of the lipid. Moreover, the compatibility of KTZ with the lipid was assessed by measuring characteristic thermal peak in DSC thermogram. The result is illustrated in figure 4A where the characteristic sharp endothermic peaks of lipid and the drug are 75.6 °C and 153.7 °C, respectively. In literature, the melting points of the lipid and KTZ were 71.7°C and 151.22°C, respectively and these results were in close agreement with the published values [18] Chemically, the used solid lipid is glycerol esters of behenic acid (C_{22}) containing behenic acid as major constituent (≅85%). Moreover, the lipid is amphiphilic (HLB ~ 2) in nature due to the presence of partial acylglycerol. It is noteworthy that the lipid has low peroxide value (6 meq O_2 Kg^{-1}) suggesting high chemical stability [18]. Therefore, this lipid was selected to load chemically challenged ketoconazole for improved solubility and chemical stability. The apparent endothermic DSC peak of the lipid was at 75.5°C and it indicated the purity of the lipid composed of pure triacyglycerols. The lipid is considered to be composed of a mixture of metastable polymorphic form when characteristic peak is obtained at 71.1°C [18]. The results of thermal enthalpy were 269.5 J/g and 486.9 J/g for the

drug and the lipid (CATO), respectively. KOF1 showed an endothermic shift to 89.39 °C and a significantly lowered heat flow of 92.26 J/g, which indicating incorporation of the drug into the lipid matrix (Figure 4A). Lower enthalpy for KOF1 indicates solubilized ketoconazole in the lipid matrix having more imperfections in the crystal lattice which can accommodate more drug content in their crystal lattice [19].

Fourier transform infrared spectroscopy (FT-IR)

It was prerequisite to assess compatibility of the drug with excipients used in the study. The result of FT-IR study has been portrayed in figure 4B wherein pure KTZ, optimized KOF1, and blank SLNs exhibited characteristic peaks. Notably, pure KTZ showed prominent stretching peaks at 1510 cm^{-1} for unsaturated hydrocarbon (C=C), 1646 cm^{-1} for carbony group, 1036 cm^{-1} for aliphatic ether, 1245 cm^{-1} for cyclic ether and 817 cm^{-1} for halogen attached with carbon (C-Cl). These values were in agreement with reported stretching [20]. A major peak retained at 2923 cm^{-1} and 2047 cm^{-1} in blank SNLs and KOF1 is due to stretching vibration of C-H group present in lipid excipient. Moreover, remarkable band from 1711-1742 cm^{-1} corresponds to carbonyl group (C=O) and from 1578-1609 cm^{-1} corresponding to unsaturated carbon (C=C) are associated with the lipid excipients of formulation [21]. In KOF1, few characteristic peaks of the drug (2962-2836 cm^{-1} assigned for C-H stretching, 1652 cm^{-1} for C=O stretching vibration), lipid (14898-1553 cm^{-1}) and other excipients were retained with slight variation in intensities. Few peaks of the drug (for C-N and C-Cl) were overlapped with the lipid [22]. This reflected compatibility of the drug with the excipients present in the formulation. The characteristic peaks present in the formulation are due to unentrapped drug outside the lipid matrix.

Powder X-ray diffraction (PXRD)

This was carried out to identify the solid state characteristic behaviour of the pure ketoconazole and developed formulation. The technique was helpful to identify crystallinity and amorphous nature of the drug and KOF1, respectively as shown in figure 4C. The lyophilized KOF1 and blank formulation were found to be amorphous as compared to pure KTZ. This confirmed that the KTZ loaded SLNs formulation was relatively soluble as compared to pure drug. KTZ exhibited remarkable peaks with 2θ values of 7.2, 17.4, 19.8, 22.2, and 24.9. These suggested the crystalline nature of the drug and were found to be complying with previous report [23]. Blank formulation revealed amorphous nature due to blend of lipid with surfactant and stabilizer. The lack of characteristic peaks of the drug in KOF1 may be due to solubilized form of KTZ in lipid matrix amalgamated completely or molecularly dispersed state of KTZ or amorphous nature [24] . Moreover, this suggested least unentrapped drug outside the lipid core.

Surface morphology analysis

FE-SEM and HR-TEM are two advanced and sophisticated technology to visualize morphological behavior of nanomedicine or nanocarrier at varied resolution and magnification. The shape and size of the particle are important aspect to assess for several confirmation. The representative images of FE-SEM and HR-TEM are presented in figure 5A-B. The high magnification (10000X) HR-TEM image

illustrated that the lipid core was enclosed with a hydrophilic firm layer of the surfactant. Acquisition of perfectly spherical shape was attributed to the mixture of surfactants mediated effective covering around the SLNs surface during homogenization. The size of SLNs observed by HR-TEM was a relatively lower than the value obtained in DLS. This variation is associated with several factors such as instrumental error of TEM (relative adsorption of smaller size particle by the grid) and the collapsed SLNs after water evaporation during drying process [25]. It is apparently observed that the optimized KTZ-SLNs (KOF1) formulation was homogeneously dispersed, discrete and spherical. In general, spherical particles are relatively stable and suitable for improved permeation across skin. Moreover, spherical particles are considered to sustain their shape upon storage while disc shaped or discoid particles tend to aggregate which lead to gelation upon storage [26] [27].

In-vitro drug release

The drug is highly crystalline in nature and poorly soluble in water (0.04 mg/ mL) or buffer. In-vitro release behaviour of the drug suspension and KOF1 (KTZ-SLNs) was determined PBS (pH 7.4) containing 5% of DMSO (maintained sink condition). It observed that the drug was poorly released (38%) across the dialysis membrane from the drug suspension over a period of 2 h and then no release was observed. There was no release after 2 h due to poor solubility of the drug. Moreover, the optimized formulation exhibited an initial burst release within 2 h due to free drug and subsequent extended release (99.84%) up to 72 h (figure 6A). KTZ release from SLNs was exponential in first 2 h followed by sustained release over 72 h which may be attributed to solid lipid matrix amalgamated with the drug. However, 35% of the total loaded drug was released within 2 h and these values closely correspond to the free/unentrapped drug present in the KTZ-SLN formulation. Free/unentrapped KTZ was released from the SLNs at a rate slower than the free drug associated with SLNs. Different kinds of kinetic release models were applied to understand the release mechanism from the lipid matrix. In first 12 h, the release mechanism followed non-Fickian as evidenced with low ‘n’ value (0.82) (Korsmeyer-Peppas model) and the applied model was the best fit (r^2= 0.9948). From 24 h to 72 h, zero order release model was the best fit model (r^2=0.9961) for KTZ-SLNs suggesting slow and controlled release from the lipid matrix. This diffusion controlled release was predicted to occur from porous matrices [28]. The release of drug from a matrix can be predicted based on the various drug release models.

Ex-vivo skin permeation

The drug permeation profile and pattern of formulations (KTZ-SLNs, KTZ SUS and KTZ-MKT) are illustrated in figure 6B. The cumulative amounts of the drug permeated across rat skin at the end of 72 h were found to be as 6643.58±210.2 µg, 2924.66±90.6 µg and 1134.14±11.3 µg for KTZ-SLNs, KTZ-MKT and KTZ-SUS respectively (figure 6B). KTZ-SLNs dispersion is known to show high skin permeation attributed to its adhesiveness and occlusiveness coupled with hydration effect [29]. The transdermal flux was the highest (after 24 h) in KTZ-SLN dispersion (134.40±4.2 µg/cm^2/h) as compared to KTZ-SUS (23.80±1.8 µg/cm^2/h) and KTZ-MKT (48.31±2.7 µg/cm^2/h), respectively. This improvement can be attributed to the presence of co-surfactant (PEG 600), which being a hydrophilic molecule, incorporated

into the polar head group of the skin lipid bilayer resulting in greater penetration of the lipid phase by solvation of the α-keratin and therefore reduces drug-tissue binding [30]. Transdermal flux value observed for KTZ-SLNs was significantly higher than the ones observed for KTZ-MKT and KTZ-SUS, which indicates that permeation of KTZ by SLNs was significantly influenced by the structural arrangement of excipients. Transdermal flux of KTZ-SLNs penetrated in the receptor medium after 72 h was very low (45.91±1.1 μg/cm^2/h). However it is evidently vivid from the results that SLNs provoked the drug access to the deeper layer of skin as the prime target site of fungal residence causing dermal infections. However, non-significant permeation flux in acceptor chamber, indicated minimum probable chance of systemic side-effects. The retentive amount of KTZ in rat skin strata was determined by skin retention study. Drug should reach and stay in deeper layer of skin for effective management of skin related fungal infections. The drug retention from KTZ-SLNs, KTZ-MKT and KTZ-SUS are shown in figure 6C. Drug concentration deposited in rat skin from KTZ-SLNs was 1383.14±90.3μg/cm^2 which was higher as compared to KTZ-SUS (303.81±48.3μg/cm^2) and KTZ-MKT (336.31±54.4 μg/cm^2). Higher drug retention of KTZ from KTZ-SLNs could be due to the lipid and the surfactant responsible to cause reversible conformational changes in skin lipid. SLN formulation carrying glyceryl behenate as main carrier has been reported to internalize with the lipid of stratum corneum and forms a reservoir of KTZ in the skin layers for sustained and extended release [31] . However, these nanoparticles may opt follicular route of the drug permeation to serve as depot reservoir [32]. Conclusively, augmented permeation and drug deposition in the deeper layer of skin may have achieved thorough combination of physiological and physicochemical mechanisms working together such as lipid-lipid interaction, skin lipid and SLNs fusion, surfactant mediated skin lipid extraction, follicular mediated SLNs transport to the dermal area, and transepidermal water loss [28].

Dermatokinetic Studies

The concentration time profile (figure 6D) and dermatokinetic parameters of KTZ-SLNs, KTZ-SUS and KTZ-MKT after topical administration were determined in rat skin. A significant higher ($p<0.001$) value of C_{max} (7.1 fold), $AUC_{0-\infty}$ (9.0 fold) and $AUMC_{0-\infty}$ (10.6 fold) for KTZ-SLNs with respect to KTZ-SUS. Furthermore KTZ-SLNs have significantly higher ($p<0.001$) C_{max} (4.1 time), $AUC_{0-\infty}$ (4.6 time) and $AUMC_{0-\infty}$ (5.6 time) with respect to KTZ-MKT. Concentration of drug in skin progressively declined to 46.32 μg/ mL after 72 h from its C_{max} value (225.19±9.5 μg/ mL) detected at 24 h. This indicating prolonged and sustained release of KTZ-SLNs in skin layers as compared to KTZ-SUS (3.8 μg/ mL) and KTZ-MKT (4.4 μg/ mL) at 72 h. It was observed that small particles size of SLN possess a high specific surface area and therefore adhesive properties by leading occlusivity due to film formation after application on the skin. Film formation prevented water evaporation from skin and penetration of KTZ-SLNs through rat skin was increased. Figure 6D presented skin concentration-time profiles of the optimized KOF1, drug suspension, and marketed formulations after topical application on rat skin. It is obvious that KOF1 improved plasma concentration of ketoconazole when tailored in solid lipid nanoparticles as compared to drug suspension and commercial product. The result suggested that the proposed nanoparticle was capable to deliver the drug to the systemic circulation which can be suitable for systemic fungal infection

control. The small particle size of SLN in the nanometer size range caused adherence to the stratum corneum (SC), consequently increased KTZ penetration into viable layer of skin onto which fungal cells reside.

Fluorescence microscopy study on human dermatome skin (EpiDerm^{TM})

To support the ex vivo permeation and drug deposition findings, this was carried out to visualize the dye loaded SLNs (KOF1) applied on the human dermatome skin (EpiDerm^{TM}) for 2 and 24 h under fluorescent microscopy. An aqueous solution of the dye served as control and applied on the same EpiDerm^{TM}. The fluorescent images are shown in figure 7. From figure 7A and 7B, the fluorescence was only detected at the skin surface in the fluorescein solution group after cultivation for 2 h and 24 h. Fluorescence displayed only little penetration from external epidermis layer after 2 h treatment (figure 7C) with fluorescein-loaded in SLNs. After 24 h of treatment, fluorescein-loaded SLNs treatment group showed appreciable fluorescence deeper inside the viable epidermis (figure 7D). SLNs are reported to permeate the skin via where they are found to accumulate resulting in a depot, subsequent release of KTZ from SLNs present in skin/hair follicles provide an effective, sustained treatment of fungal infection [25] [33].

Vibrational spectroscopy imaging of human skin

ATR-FTIR imaging on skin cross section

Human skin cross-sections were recorded by ATR-FTIR imaging spectroscopy. Figure 8 shows visible images of a skin cross-section and the associated hyperspectral image. The method allowed to investigate and visualize the penetration of KTZ of KTZ-SLNs and other SLN components in the integral epidermis. The FTIR Imaging System recorded hyperspectral images which provide maps showing the co-localization of specific molecular components (KTZ or SLN components). These images were generated with false colours where the red represent highest values and the blue the lowest values for each parameter investigated. The ratio between 816 cm^{-1} (C-Cl) to Amide I band area was used to follow the penetration of KTZ while the ratio between 945 cm^{-1} to Amide I band area was used to follow the penetration of SLN components. Indeed, the band around 816 cm^{-1} is specific of the KTZ while the band around 945cm^{-1} is specific of the SLN components (Figure 9).

The SLNs penetration will allow the release of KTZ inside the human skin samples when they will exhibit polymorphosize from β to β', a more stable crystalline form. Peak for both KTZ and SLN components is observed deep inside the epidermis (Figure 9). The ATR-FTIR images in the Figure 10 show clearly that SLNs penetrated inside the human skin, the maximum penetration was reached after 24h of treatment. After 24h, the SLNs had penetrated up to the deepest part of the epidermis.

Confocal Raman spectroscopy imaging

The FTIR data were confirmed by Confocal Raman spectroscopy. The Confocal Raman images in the figure 11 clearly show that SLNs penetrated the stratum corneum in the first 3h and reached the viable epidermis after 24h. There was a nice co-localization of the KTZ and the SLNs inside the human skin samples. Indeed, like the SLNs the KTZ penetrated the stratum corneum in the first 2 h and reached the deeper part of the epidermis after 24 h.

Long term stability

Nanoparticles are associated with instability due to physical and chemical factors such as particulate aggregation, size variation and drug content under varied temperature and humidity. Therefore, it is essential parameter to estimate shelf life of a product or success of the product to comply regulatory condition before approval or marketing. Particle size, %EE, and the drug content were estimated over different temperature, humidity and time period as shown in figure 12. The PS of KTZ-SLN stored at 4^0C±1.0 ^{0}C, 30°C ± 2°C/65± 5% RH and 40°C ± 2°C/75± 5%RH ranged as 236.8±16.7 - 565.2±20.5 nm, 336.8±16.7 - 658.7±98.5 and 336.8±16.7 - 1346.98±133.1 respectively. Particle growth was slower at 4±1.5^{0}C than when stored at higher temperatures. Kinetic energy of the system increases at higher temperatures, yielding aggregates (and hence increase in size) due to higher frequency of collisions between particles [34,35]. Microviscosity (the friction experienced by particles) is a temperature dependent factor and decreases with an increase in temperature leading to particle destabilization and possibly agglomeration [36]. The %EE of KTZ-SLNs stored at 4^0C±1.5^{0}C, 30°C ± 2°C/65% RH ranged between 87.5±3.2–81.2±0.7% and 87.5±3.2–73.5±1.9% respectively. The corresponding drug assay (% TDC) for KTZ-SLNs ranged between 94.9±1.7–87.90±0.6% and between 94.9±1.7–80.5±0.8%, respectively. The %EE and %TDC of KTZ-SLNs stored at 40°C ± 2°C/75% RH ± 5% RH ranged between 87.5±3.2–19.3±1.1% and 94.9±1.7–24.92±1.7% respectively. High temperatures (40± 2°C/75± 5% RH) facilitate transformation of lipid into various metastable polymorphic states which results in drug expulsion and leaching. A transformation of SLN from β$^/$ to β form resulting in drug expulsion (as indicated by significantly decreased EE) [37]. The investigated drug is also associated with light mediated instability. Interestingly, the total drug content (% TDC) was found to be reduced under UV light ($p \leq 0.05$; figure 8D-E) in drug suspension at the end of 10 days. In contrast, %TDC remained was substantially high in SLNs at the end of 10 days. KTZ-SUS showed a significant ($p < 0.001$) reduction in %TDC (remained drug as 66.4%) when stored in the transparent glass vial as compared to amber glass (remained drug content as 30.3%). This was also inspected for visual examination. The drug content stored in transparent glass turned to slightly pink colour upon storage (suspension) whereas KTZ-SLNs retained their white colour. This may be prudent to correlate with high protective nature of compritol possessing low value of peroxide value as mentioned before [38].

Conclusion

Ketoconazole is a potential established antifungal drug with limited aqueous solubility and poor topical efficacy in conventional dosage form. Commercial cream available is also challenged for limited clinical

efficacy on topical application and oral delivery to control resistant and recurrence cases. In literature, various topical and transdermal formulations have been reported for improved efficacy based on overestimated data of in vitro findings. Therefore, we addressed solid lipid nanoparticle with optimum level of compritol and tween 80 to achieve desired size, % EE and %TDC. Ex vivo permeation and drug deposition findings were further supported with fluorescence microscopy study using human cadaver skin model after topical application. It was important to investigate and assess in human skin model (cadaver) for mechanistic and tangible degree of permeation across the crystalline barrier (stratum corneum). Moreover, in vivo dermatokinetics data assured that the approach was capable to access the drug to the dermal region in substantial concentration with limited transport to systemic circulation. Vibrational imaging spectroscopies techniques used as proof of concept as KTZ-SLNs were confirmed to penetrate up to the viable epidermis human skin. Finally, long term stability and photostability data indicated protective benefits of compritol used in the formulation. Thus, the compritol based SNLs was promising carrier for improved permeation, drug deposition, penetration, dermatokinetics parameters, and increased stability over long period.

Declarations

Ethics approval and consent to participate

All animal experiments are conducted after obtaining ethical approval from the Institutional Animal Ethics Committee of Panjab University, Chandigarh (PU/45/99/CPCSEA/IAEC/2018/150)

Consent for publication

All the authors agreed with the content and gave explicit consent to submit the work.

Availability of data and materials

The data generated during the study is provided in the manuscript and is available from corresponding authors on reasonable request.

Funding

There is no funds given by any funding agency

Competing interests

The authors declare no competing interests

Author's contribution

Mohhammad Ramzan: Manuscript writing and drafting, Samuel Gourion-Arsiquaud: Permeation studies using vibrational spectroscopy, review & editing, Afzal Hussain: Manuscript editing and review, Jaspreet Singh Gulati: Supply of materials, study protocol, Qihong Zhang: Vibrational spectroscopic studies, Sonia

Trehan: Fluorescent microscopic studies, Vinam Puri: Analytical method development, Bozena Michniak-Kohn: Methodology, data curation and reviewing. Indu Pal Kaur: Conceptualization review & editing

Acknowledgments

The authors acknowledge the UGC-CAS, DST-FIST and PURSE funded facility of UIPS, Panjab University, India used for characterization of KTZ-SLNs; SAIF facility of DST at Panjab University Chandigarh, India; TRI Princeton and Centre for Dermal Research, New Jersey, USA for conduct of permeation studies, ATR-FTIR and Confocal Raman spectroscopy studies.

References

1. Hainer BL. Dermatophyte infections. Am Fam Physician. 2003;67:101–8.
2. Ameen M. Epidemiology of superficial fungal infections. Clin Dermatol. 2010;28:197–201. https://doi.org/10.1016/j.clindermatol.2009.12.005.
3. Choi FD, Juhasz ML, Mesinkovska NA. Topical ketoconazole: A systematic review of current dermatological applications and future developments. J Dermatolog Treat. 2019;30:760–71. https://doi.org/10.1080/09546634.2019.1573309.
4. Logua AD, Faddab AM, Anchisib C, et al. Effects of in-vitro activity of miconazole and ketoconazole in phospholipid formulations. J Antimicrob Chemother. 1997;40:889–93. https://doi.org/10.1093/jac/40.6.889.
5. FDA. Drug Safety Podcast. Acesssed, November 09, 2020 https://www.fda.gov/Drugs/DrugSafety/DrugSafetyPodcasts/ucm504300.htm 2010.
6. Guo F, Wang J, Ma M, et al. Skin targeted lipid vesicles as novel nano-carrier of ketoconazole: characterization, in vitro and in vivo evaluation. J Mater Sci Mater Med. 2015;26:175. https://doi.org/10.1007/s10856-015-5487-2.
7. Patil PR, Biradar SV, Paradkar AR. Extended release felodipine self-nanoemulsifying system. AAPS PharmSciTech. 2009;10:515–23. https://doi.org/10.1208/s12249-009-9235-0.
8. Kakkar S, Karuppayil SM, Raut JS, et al. Lipid-polyethylene glycol based nano-ocular formulation of ketoconazole. Int J Pharm. 2015;495:276–89. https://doi.org/10.1016/j.ijpharm.2015.08.088.
9. Das S, Ng WK, Kanaujia P, et al. Formulation design, preparation and physicochemical characterizations of solid lipid nanoparticles containing a hydrophobic drug: Effects of process variables. Colloids Surf B. 2011;88:483–9. https://doi.org/10.1016/j.colsurfb.2011.07.036.
10. Hu L, Tang X, Cui F. Solid lipid nanoparticles (SLNs) to improve oral bioavailability of poorly soluble drugs. J Pharm Pharmacol. 2004;56:1527–35. https://doi.org/10.1211/0022357044959.
11. Hussain A, Samad A, Nazish I, et al. Nanocarrier-based topical drug delivery for an antifungal drug. Drug Dev Ind Pharm. 2014;40:527–41. https://doi.org/10.3109/03639045.2013.771647.
12. Hussain A, Samad A, Singh S, et al. Enhanced stability and permeation potential of nanoemulsion containing sefsol-218 oil for topical delivery of amphotericin B. Drug Dev Ind Pharm. 2014;41.

13. Barry BW. Mode of action of penetration enhancers in human skin. J Control Release. 1987;6:85–97. https://doi.org/10.1016/0168-3659(87)90066-6.
14. Abioye AO, Issah S, Kola-Mustapha AT. Ex vivo skin permeation and retention studies on chitosan–ibuprofen–gellan ternary nanogel prepared by in situ ionic gelation technique—a tool for controlled transdermal delivery of ibuprofen. Int J Pharm. 2015;490:112–30. https://doi.org/10.1016/j.ijpharm.2015.05.030.
15. ICH. Q1B Photostability Testing of New Drug Substances and Products. Accessed on Feb, 12. 2020 https://www.fda.gov/regulatory-information/search-fda-guidance-documents/q1b-photostability-testing-new-drug-substances-and-products.
16. ICH. Q1A (R2). Stability Testing of New Drug Substances and Products. Accessed on Feb, 25, 2021 https://www.fda.gov/regulatory-information/search-fda-guidance-documents/q1ar2-stability-testing-new-drug-substances-and-products.
17. Iester M, Orsoni GJ, Gamba G, et al. Improvement of the ocular surface using hypotonic 0.4% hyaluronic acid drops in keratoconjunctivitis sicca. Eye. 2000;14:892–8. https://doi.org/10.1038/eye.2000.244.
18. Souto EB, Mehnert W, Müller RH. Polymorphic behaviour of Compritol®888 ATO as bulk lipid and as SLN and NLC. J Microencapsul. 2006;23:417–33. https://doi.org/10.1080/02652040600612439.
19. Müller RH, Runge S, Ravelli V, et al. Oral bioavailability of cyclosporine: Solid lipid nanoparticles (SLN®) versus drug nanocrystals. Int J Pharm. 2006;317:82–9. https://doi.org/10.1016/j.ijpharm.2006.02.045.
20. Karolewicz B, Górniak A, Owczarek A, et al. Thermal, spectroscopic, and dissolution studies of ketoconazole–Pluronic F127 system. J Therm Anal Calorim. 2014;115:2487–93.
21. Tatke A, Dudhipala N, Janga KY, et al. In situ gel of triamcinolone acetonide-loaded solid lipid nanoparticles for improved topical ocular delivery: Tear kinetics and ocular disposition studies. Nanomaterials. 2018;9:33. https://doi.org/10.3390/nano9010033.
22. Vieira IRS, Miranda GdS, Ricci-Júnior E, et al. Waterborne poly(urethane-urea)s films as a sustained release system for ketoconazole. e-Polymers. 2019;19:168–80. https://doi.org/10.1515/epoly-2019-0018.
23. Vasoya J, Shah A, Serajuddin A. Investigation of possible solubility and dissolution advantages of cocrystals, I: Aqueous solubility and dissolution rates of ketoconazole and its cocrystals as functions of pH. ADMET DMPK. 2019;7:106. https://doi.org/10.5599/admet.661.
24. Dudhipala N, Ay AA. Amelioration of ketoconazole in lipid nanoparticles for enhanced antifungal activity and bioavailability through oral administration for management of fungal infections. Chem Phys Lipids. 2020;232:104953. https://doi.org/10.1016/j.chemphyslip.2020.104953.
25. Deng P, Teng F, Zhou F, et al. Y-shaped methoxy poly (ethylene glycol)-block-poly (epsilon-caprolactone)-based micelles for skin delivery of ketoconazole: in vitro study and in vivo evaluation. Mater Sci Eng C. 2017;78:296–304. https://doi.org/10.1016/j.msec.2017.04.089.

26. Jores K, Mehnert W, Drechsler M, et al. Investigations on the structure of solid lipid nanoparticles (SLN) and oil-loaded solid lipid nanoparticles by photon correlation spectroscopy, field-flow fractionation and transmission electron microscopy. J Control Release. 2004;95:217–27. https://doi.org/10.1016/j.jconrel.2003.11.012.
27. de Jesus MB, Zuhorn IS. Solid lipid nanoparticles as nucleic acid delivery system: Properties and molecular mechanisms. J Control Release. 2015;201:1–13. https://doi.org/10.1016/j.jconrel.2015.01.010.
28. Fu Y, Kao WJ. Drug release kinetics and transport mechanisms of non-degradable and degradable polymeric delivery systems. Expert Opin Drug Deliv. 2010;7:429–44. https://doi.org/10.3390/nano9010033.
29. Wissing SA, Müller RH. Cosmetic applications for solid lipid nanoparticles (SLN). Int J Pharm. 2003;254:65–8. https://doi.org/10.1016/S0378-5173(02)00684-1.
30. Casiraghi A, Di Grigoli M, Cilurzo F, et al. The influence of the polar head and the hydrophobic chain on the skin penetration enhancement effect of poly(ethylene glycol) derivatives. AAPS PharmSciTech. 2012;13:247–53. https://doi.org/10.1208/s12249-011-9745-4.
31. Jensen LB, Petersson K, Nielsen HM. In vitro penetration properties of solid lipid nanoparticles in intact and barrier-impaired skin. Eur J Pharm Biopharm. 2011;79:68–75. https://doi.org/10.1016/j.ejpb.2011.05.012.
32. Chen H, Chang X, Du D, et al. Podophyllotoxin-loaded solid lipid nanoparticles for epidermal targeting. J Control Release. 2006;110:296–306. https://doi.org/10.1016/j.jconrel.2005.09.052.
33. Knorr F, Lademann J, Patzelt A, et al. Follicular transport route–Research progress and future perspectives. Eur J Pharm Biopharm. 2009;71:173–80. https://doi.org/10.1016/j.ejpb.2008.11.001.
34. Hu F-Q, Jiang S-P, Du Y-Z, et al. Preparation and characteristics of monostearin nanostructured lipid carriers. Int J Pharm. 2006;314:83–9. https://doi.org/10.1016/j.ijpharm.2006.01.040.
35. Wissing SA, Kayser O, Müller RH. Solid lipid nanoparticles for parenteral drug delivery. Adv Drug Deliv Rev. 2004;56:1257–72. https://doi.org/10.1016/j.addr.2003.12.002.
36. Heurtault B, Saulnier P, Pech B, et al. Physico-chemical stability of colloidal lipid particles. Biomaterials. 2003;24:4283–300. https://doi.org/10.1016/S0142-9612(03)00331-4.
37. Das S, Ng WK, Tan RBH. Are nanostructured lipid carriers (NLCs) better than solid lipid nanoparticles (SLNs): Development, characterizations and comparative evaluations of clotrimazole-loaded SLNs and NLCs? Eur J Pharm Sci. 2012;47:139–51. https://doi.org/10.1016/j.ejps.2012.05.010.
38. Souto EB, Müller RH. SLN and NLC for topical delivery of ketoconazole. J Microencapsul. 2005;22:501–10. https://doi.org/10.1080/02652040500162436.

Figures

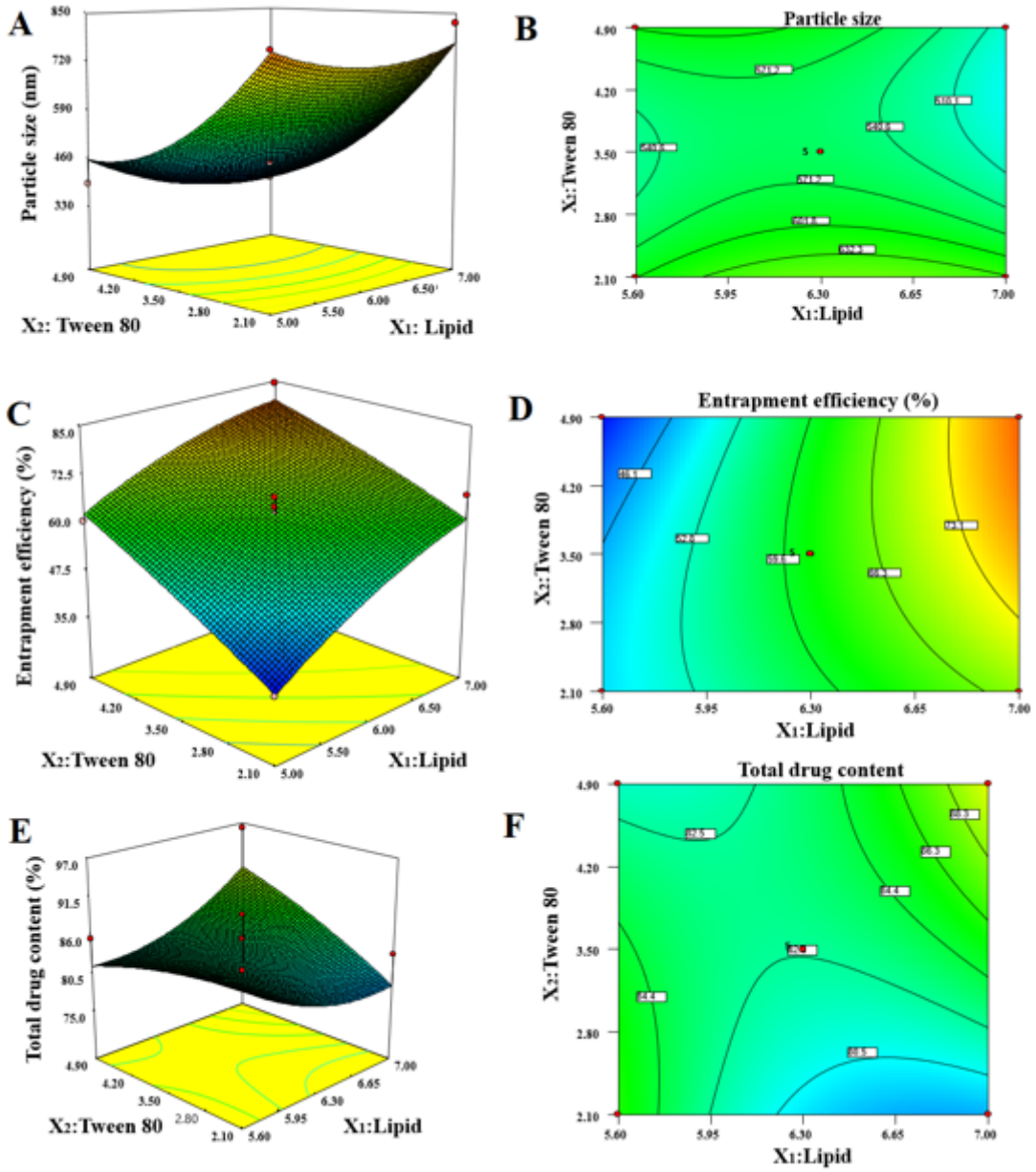

Figure 1

3-dimensional response surface and 2-dimensionl contour plots showing the influence of compritol ATO 888 (lipid) and tween 80 (surfactant) on particle size (Y1) (A-B), %EE (Y2) (C-D), and % total drug content (Y3) (E-F).

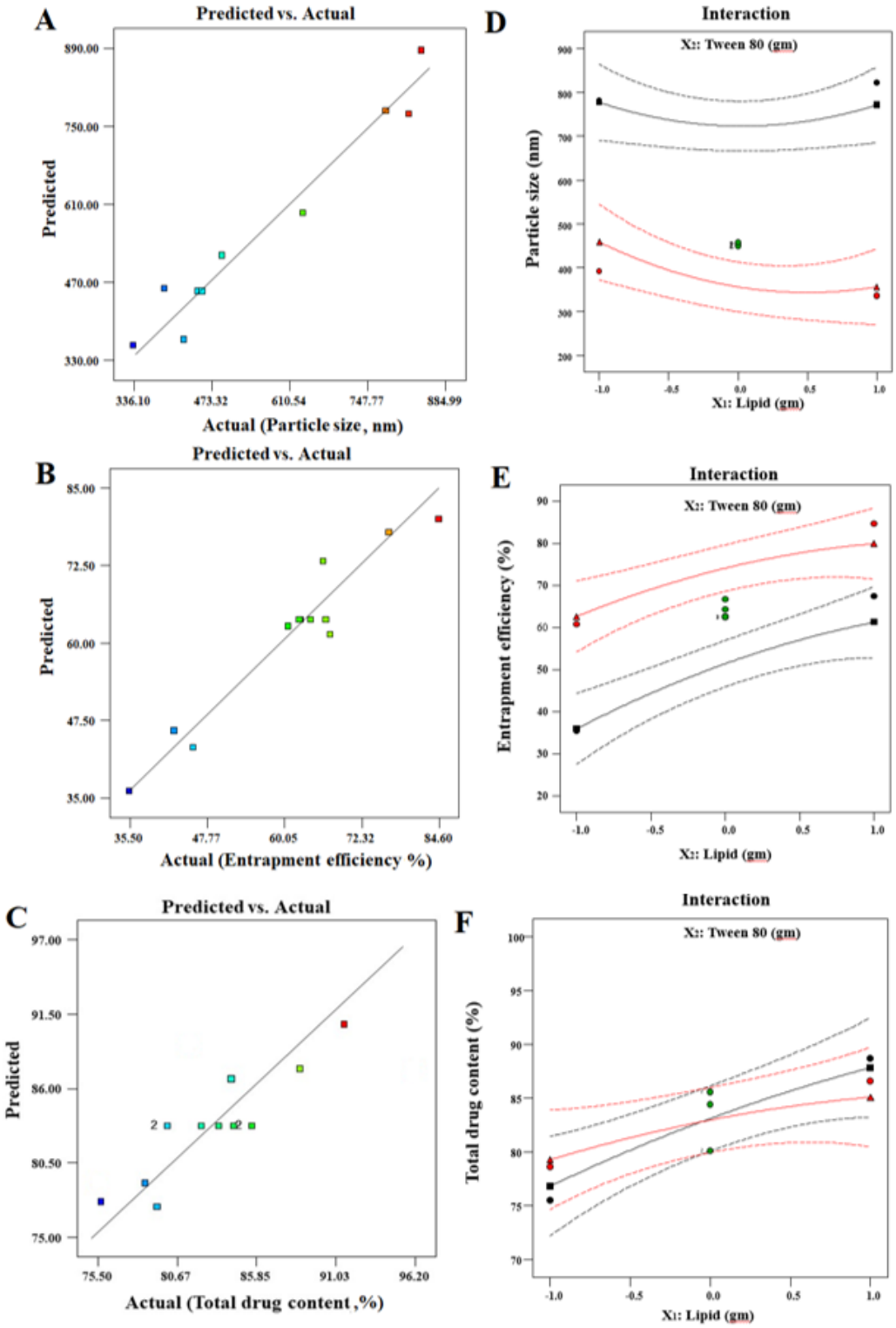

Figure 2

Predicted and observed values of responses Y1-Y3 (A-C) and interaction curves (D-F).

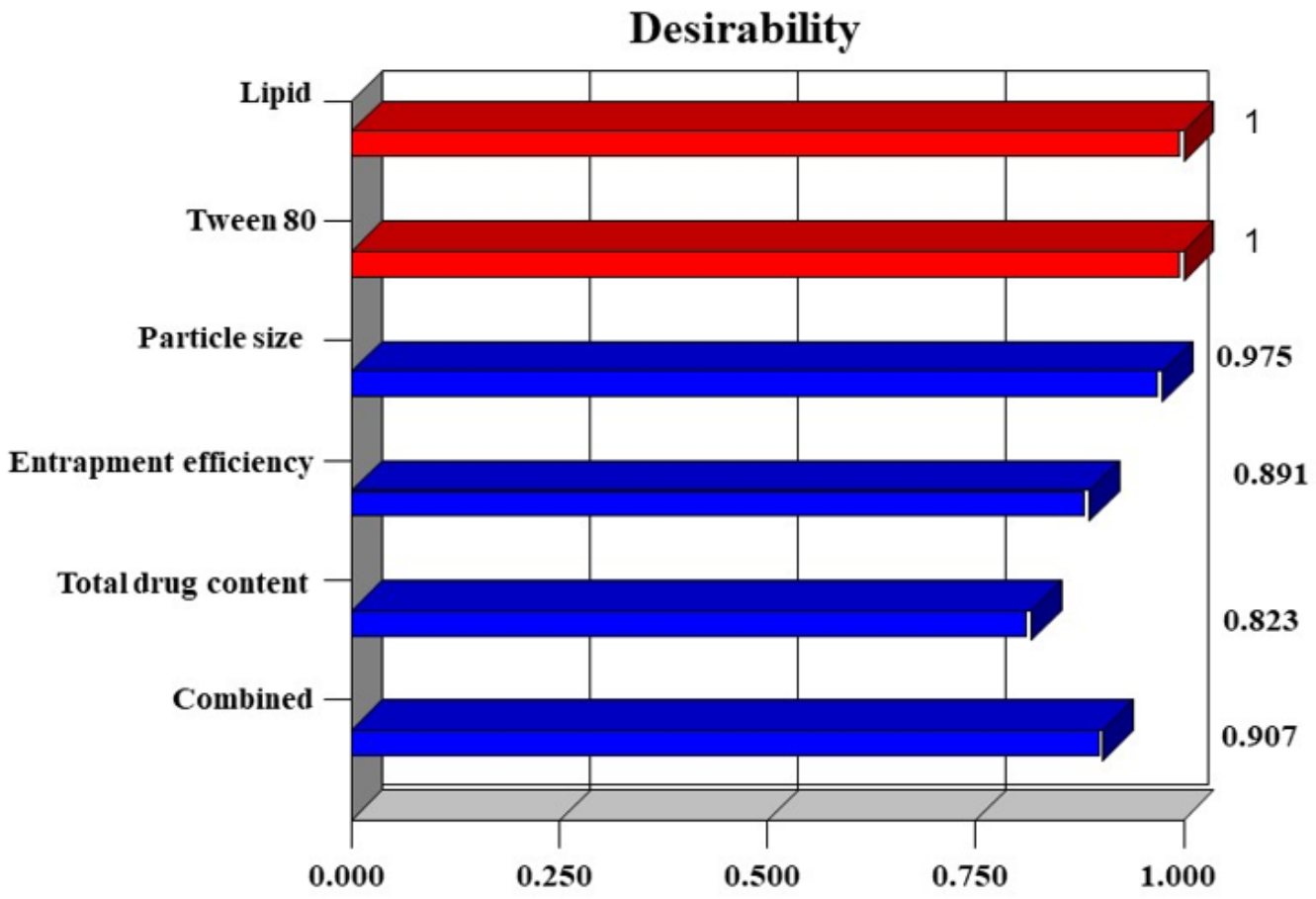

Figure 3

Desirability function parameter for the optimized KOF1

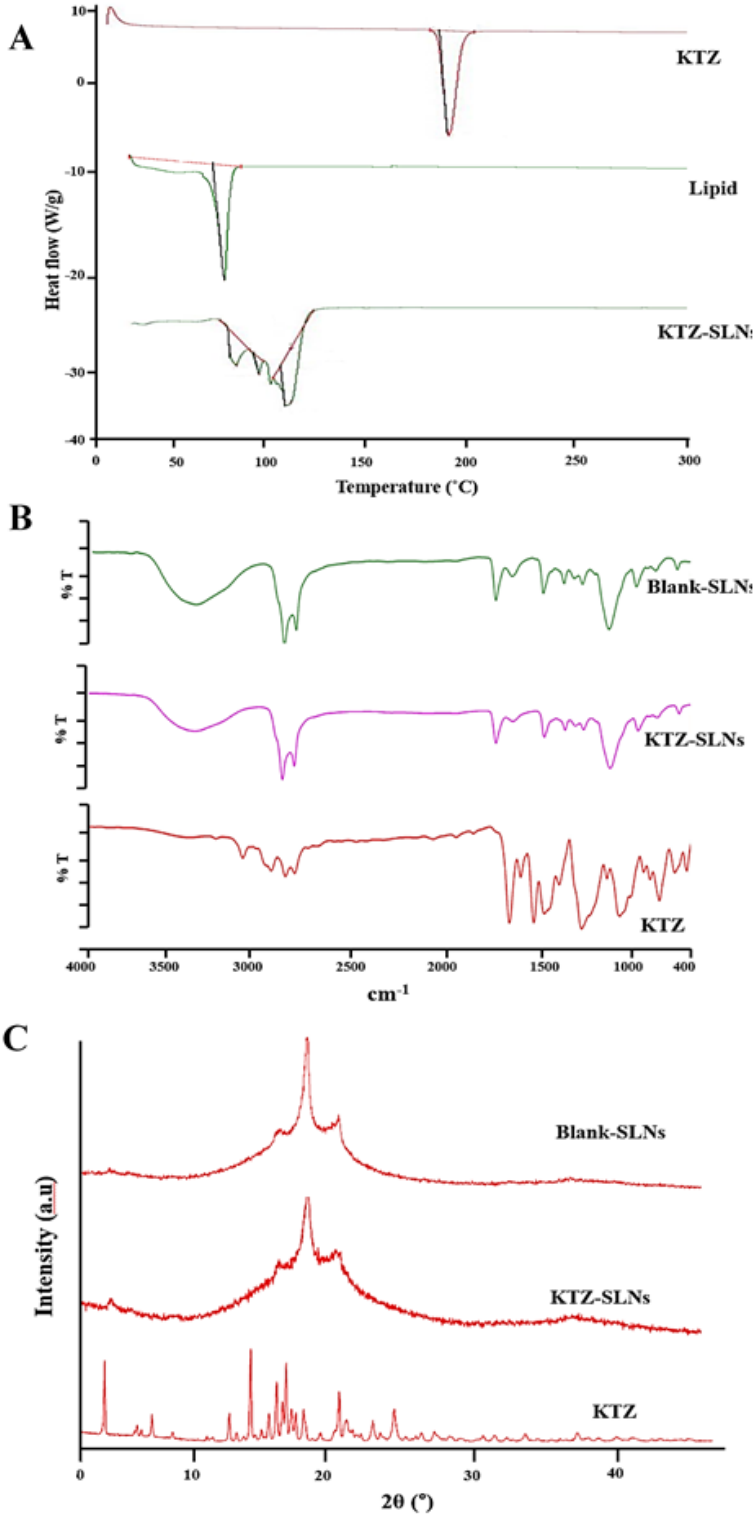

Figure 4

Evaluation of optimized formulation, blank formulation and pure KTZ: (A) DSC thermogram, (B) FT-IR spectra, and (C) Powder X-Ray diffraction study.

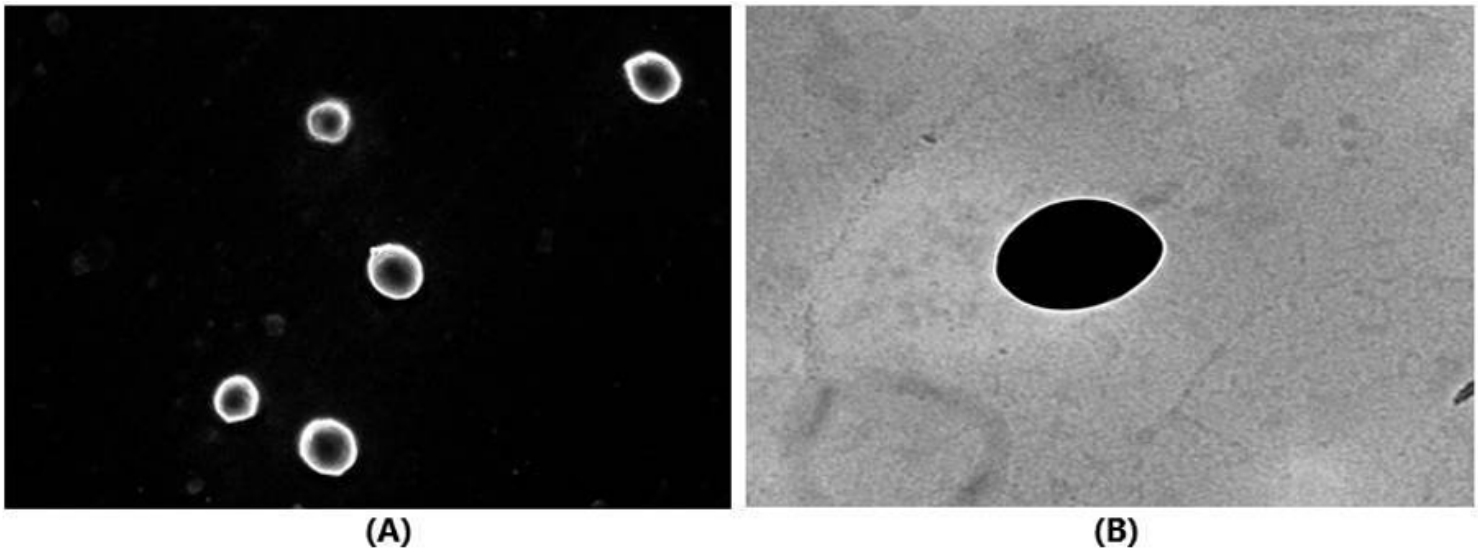

Figure 5

KTZ-SLNs (KOF1) under FE-SEM at 5000X (A) and HR-TEM at 10000X (B)

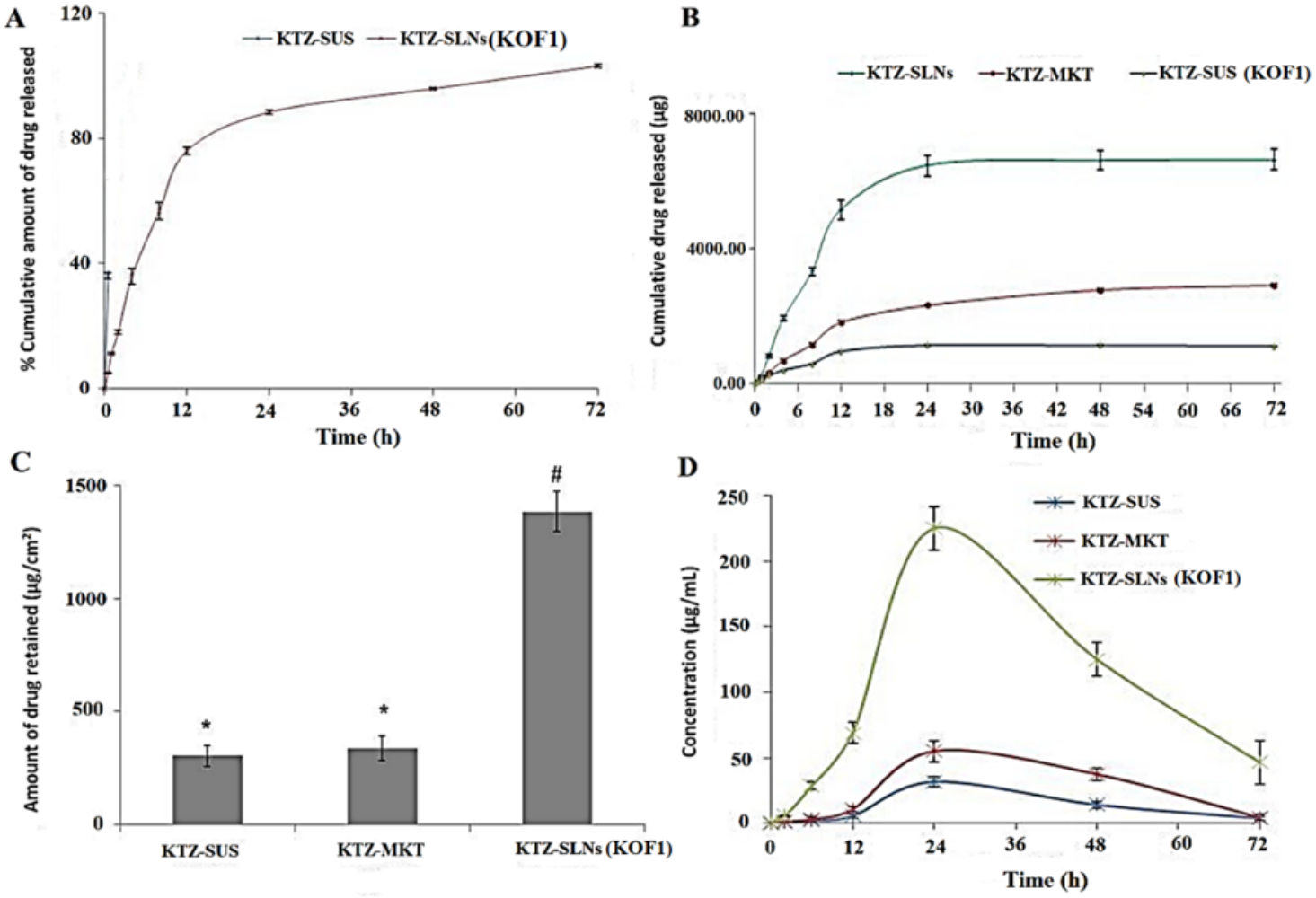

Figure 6

(A) In-vitro drug release of KTZ and KTZ-SLNs after 72 h, (B) Ex-vivo drug permeation study across rat skin illustrative description of drug permeated from across KTZ-SLNs (KOF1), KTZ-SUS and KTZ-MKT rat skin placed between a donor and receiver chamber of the Franz diffusion cell, (C) Amount of drug retained per cm2 into the rat skin after an ex-vivo permeation study of KTZ-SLNs (KOF1), KTZ-SUS and KTZ-MKT, (D) Skin concentration-time profile of KTZ-SLNs (KOF1), KTZ-MKT and KTZ-SUS following topical application to rat skin (n=6)

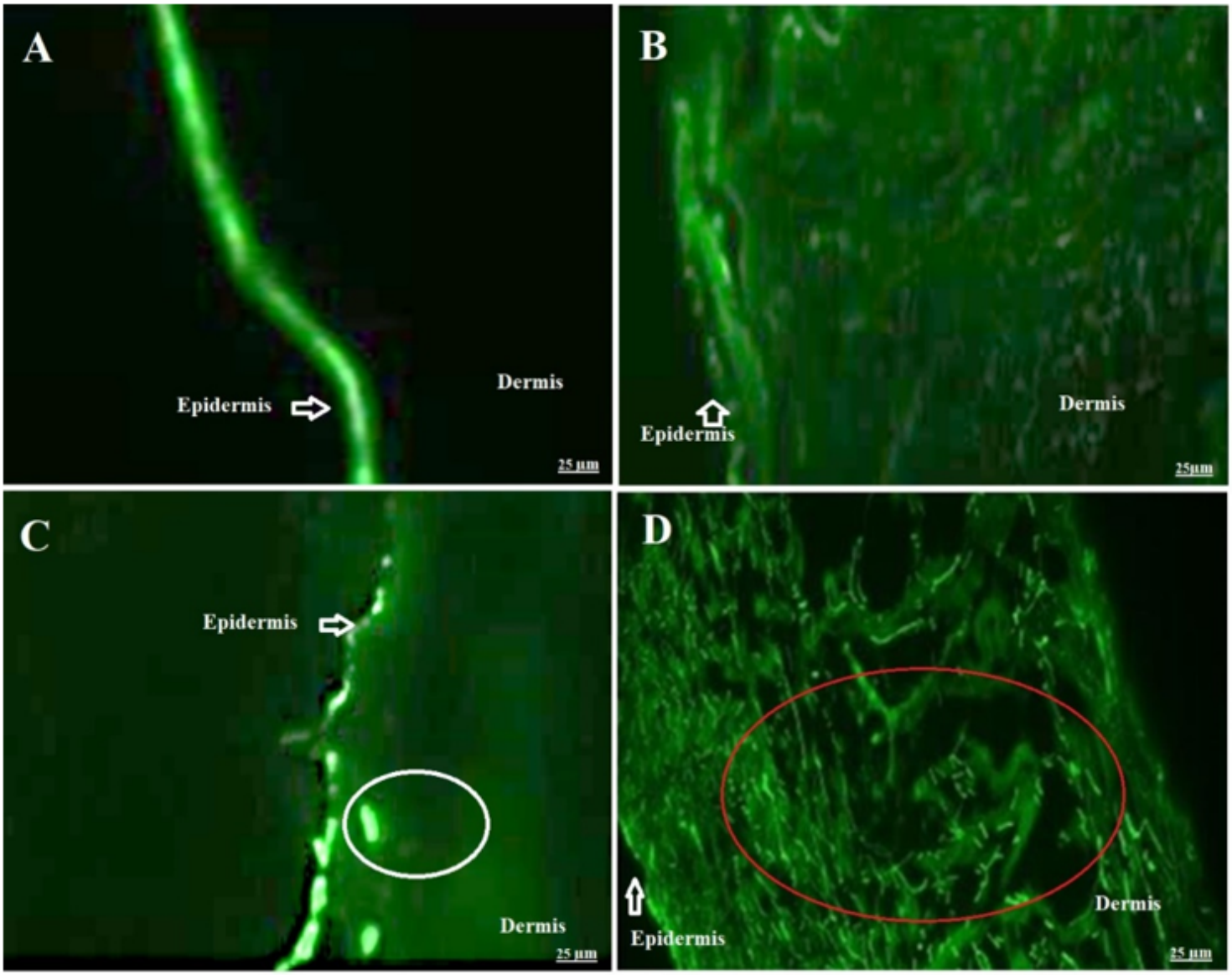

Figure 7

Fluorescent images of skin tissue (A) F-Sol 2 h, (B) F-Sol 24 h, (C) F-SLNs 2 h, (D) F-SLNs 24 h

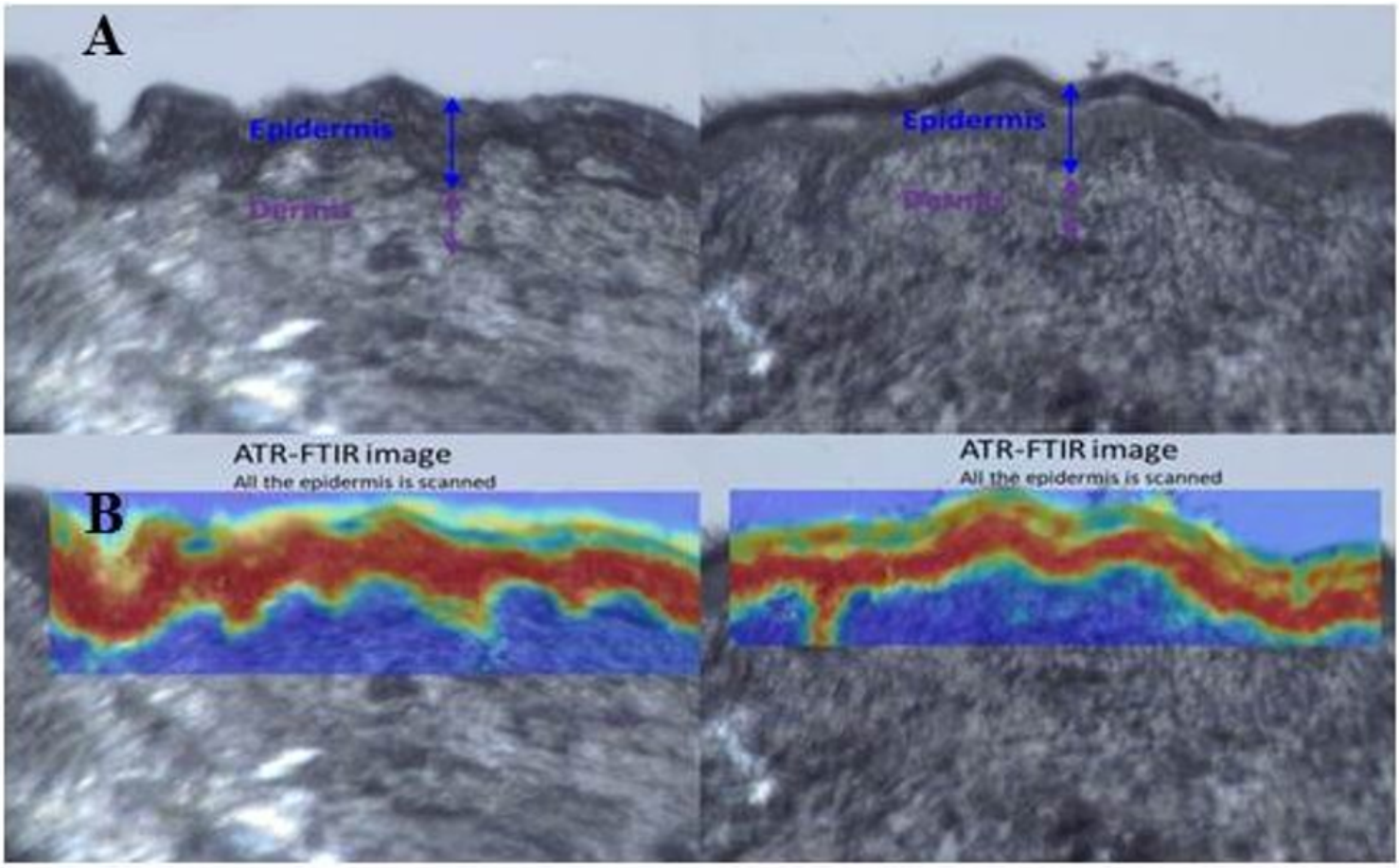

Figure 8

(A) Visible image of skin cross-section showing the epidermis and dermis region (B) Hyperspectral FTIR images superimposed on the visible image indicating the whole epidermis was scanned

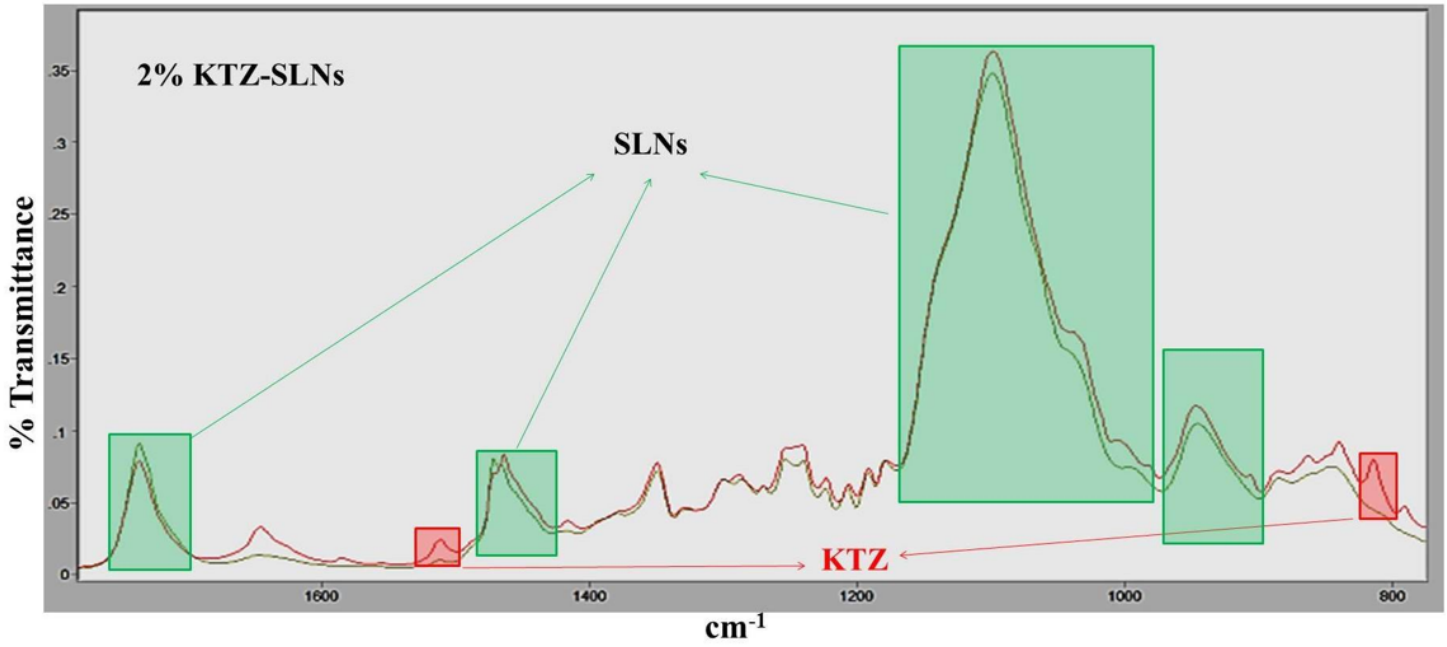

Figure 9

Typical FTIR spectra recorded with 2% KTZ-SLNs. FTIR bands specific of SLN contribution are represented by the green rectangles while the bands specific of the KTZ are shown by the red rectangles in the spectra.

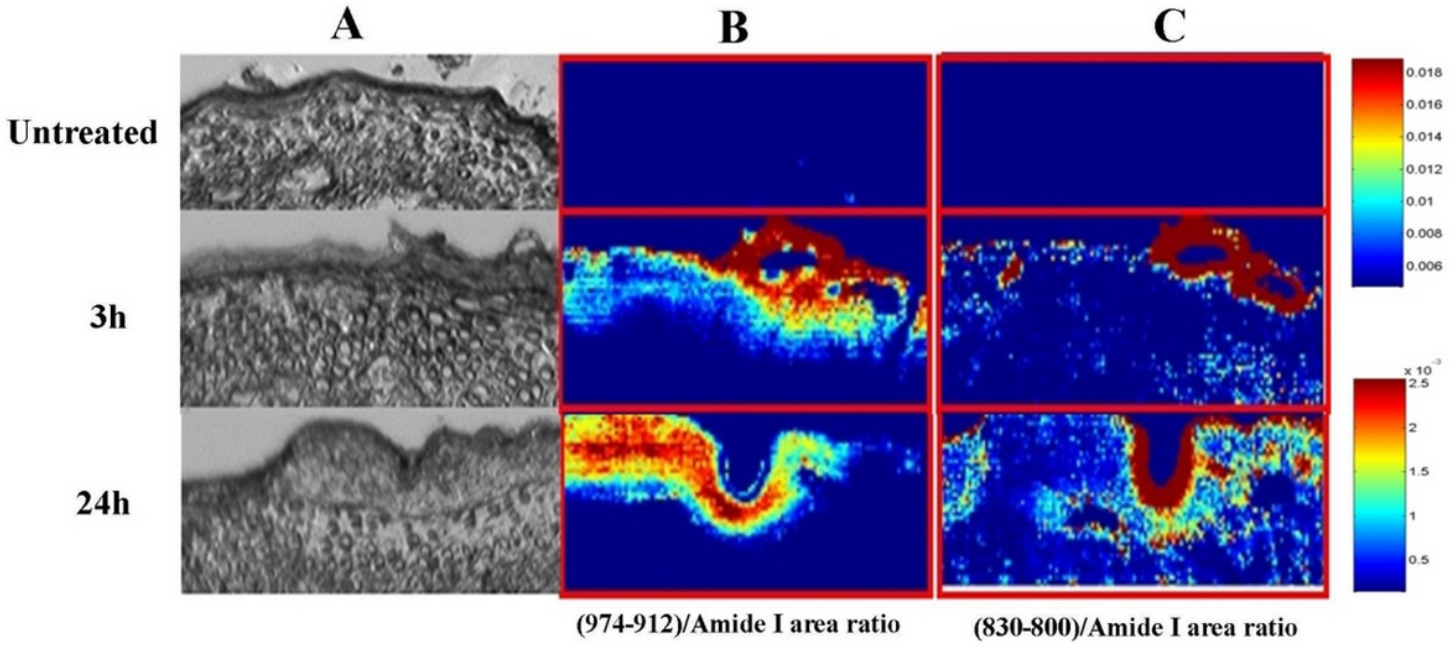

Figure 10

(A) Visible images of skin cross sections (stratum corneum on the top) (B) ATR-FTIR image of KTZ-SLNs penetration into the skin, obtained from the ratio between 945 cm-1 to Amide I peak area (representative of SLN components) and (C) ATR-FTIR image of KTZ-SLNs penetration into the skin, obtained from the ratio of the peak areas at 816 cm-1 to Amide I (representative of KTZ) peak area. Highest to lowest concentration of each component is displayed by the color scale from red (highest) to blue (lowest) as shown.

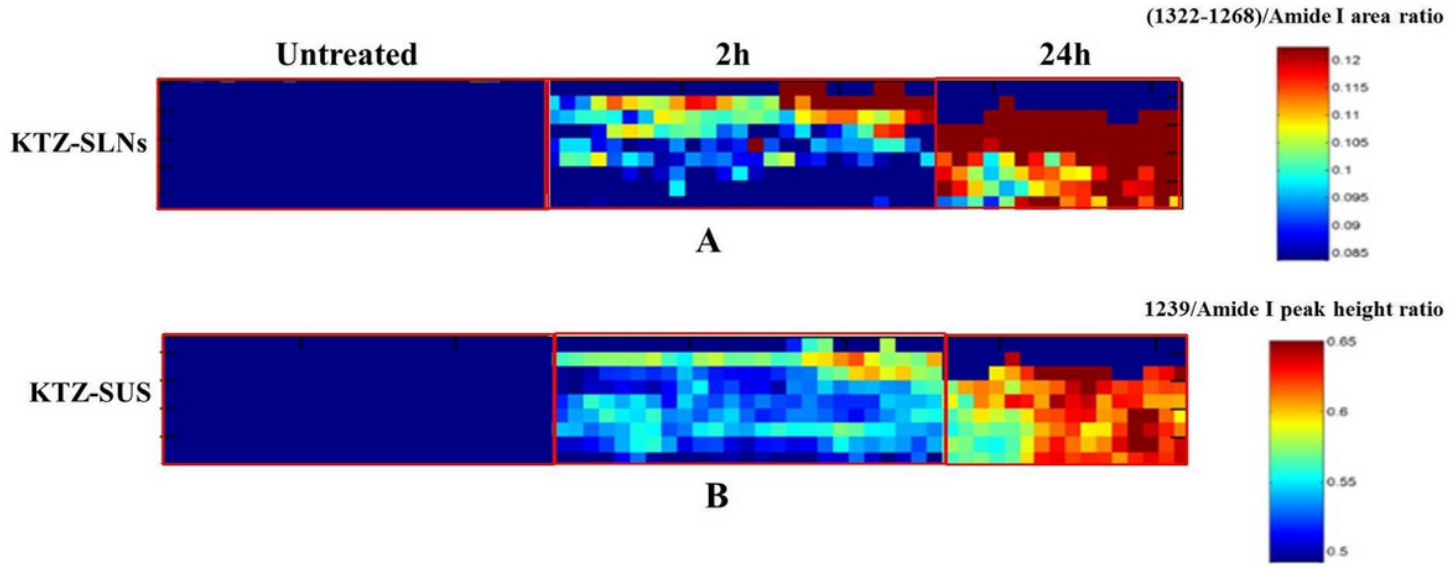

Figure 11

Confocal Raman images showing that SLNs have penetrated inside human skin treated with (A) KTZ-SLNs (B) KTZ-SUS for 2h and 24h. Highest to lowest concentration of each component is displayed by the color scale from red (highest) to blue (lowest/no component) as shown

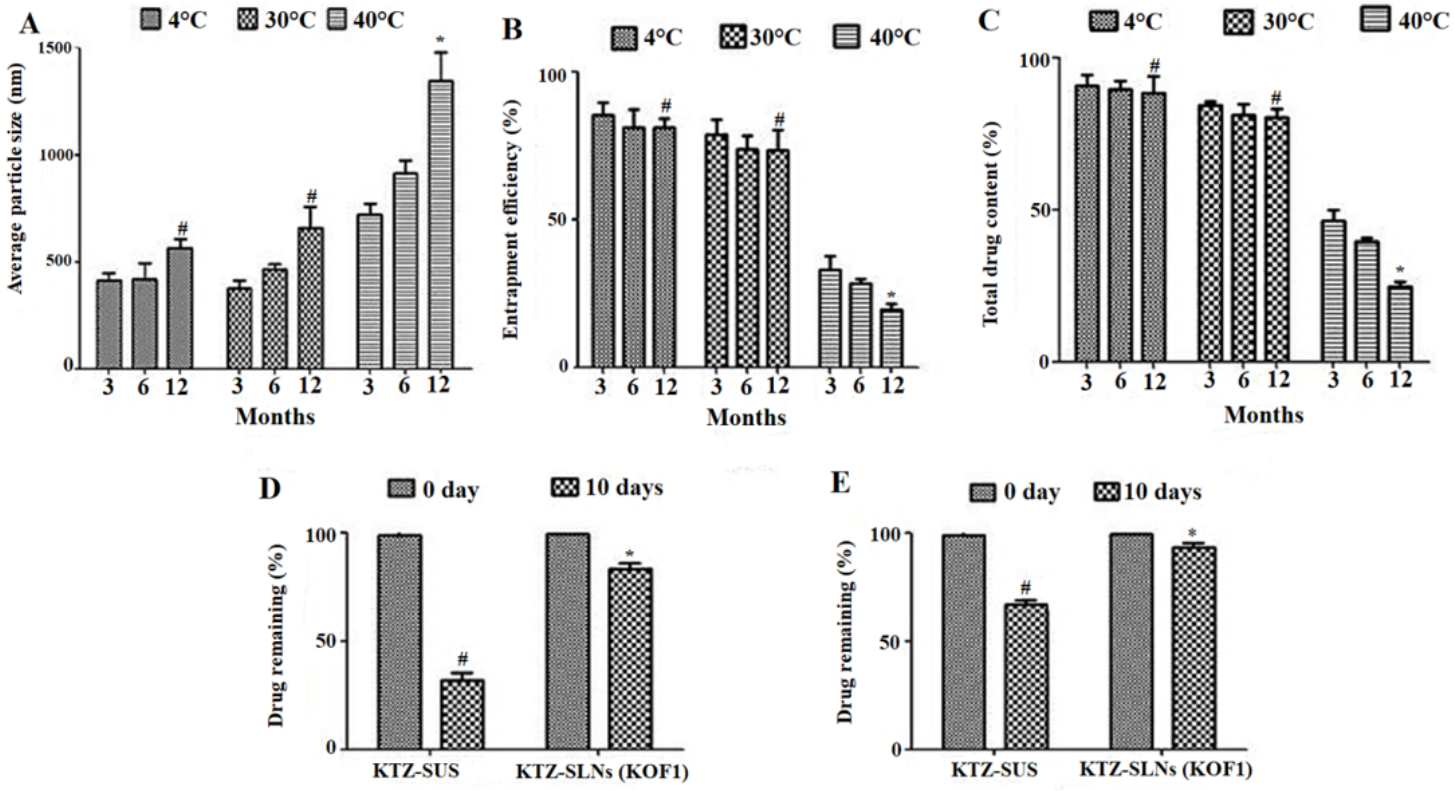

Figure 12

Effect of different temperatures on particle size (A), %EE (B), % total drug content (C) in long term stability studies. Effect of UV light on KTZ-SLNs (KOF1) & KTZ-SUS in amber colour glass (D) and transparent glass (E).

Supplementary Files

This is a list of supplementary files associated with this preprint. Click to download.

- Graphicalabstract.png